Tuning alpha rhythms to shape conscious visual perception

Published Version:
Tuning alpha rhythms to shape conscious visual perception / Di Gregorio F.; Trajkovic J.; Roperti C.; Marcantoni E.; Di Luzio P.; Avenanti A.; Thut G.; Romei V.. - In: CURRENT BIOLOGY. - ISSN 0960-9822. - STAMPA. - 32:5(2022), pp. 988-998. [10.1016/j.cub.2022.01.003]

Availability:
This version is available at: https://hdl.handle.net/11585/879206 since: 2022-03-22

Published:

DOI: http://doi.org/10.1016/j.cub.2022.01.003

Di Gregorio, F., Trajkovic, J., Roperti, C., Marcantoni, E., Di Luzio, P., Avenanti, A., Thut, G., & Romei, V. (2022). Tuning alpha rhythms to shape conscious visual perception. *Current Biology*, 32(5), 988-998.e6.

The final published version is available online at: https://doi.org/10.1016/j.cub.2022.01.003

ARTICLE TITLE: **Tuning alpha rhythms to shape conscious visual perception**

Article type: Article

Authors: Francesco Di Gregorio[1*], Jelena Trajkovic[2*], Cristina Roperti[2], Eleonora Marcantoni[2], Paolo Di Luzio[2], Alessio Avenanti[2,3], Gregor Thut[4], Vincenzo Romei[2,5]

Journal: Current Biology

Funding: V.R. is supported by BIAL foundation (204/18).

DOI: 10.1016/j.cub.2022.01.003

Tuning alpha rhythms to shape conscious visual perception

Francesco Di Gregorio[1*], Jelena Trajkovic[2*], Cristina Roperti[2], Eleonora Marcantoni[2], Paolo Di Luzio[2], Alessio Avenanti[2,3], Gregor Thut[4], Vincenzo Romei[2,5]

[1] UO Medicina riabilitativa e neuroriabilitazione, Azienda Unità Sanitaria Locale, via Castiglione 29, 40139, Bologna, Italy;

[2] Centro studi e ricerche in Neuroscienze Cognitive, Dipartimento di Psicologia, Alma Mater Studiorum – Università di Bologna, Campus di Cesena, via Pavese 50, 47521, Cesena, Italy;

[3] Centro de Investigación en Neuropsicología y Neurociencias Cognitivas, Universidad Católica del Maule, Av San Miguel, 346000, Talca, Chile;

[4] Centre for Cognitive Neuroimaging, School of Psychology and Neuroscience, University of Glasgow, 56-64 Hillhead Street, G12 8QB, Glasgow, UK;

[5] IRCCS Fondazione Santa Lucia, Via Ardeatina, 306/354, 00179, Roma, Italy.

*Equally contributed

Corresponding author and Lead Contact: mail to vincenzo.romei@unibo.it (VR)
Centro studi e ricerche in Neuroscienze Cognitive, Dipartimento di Psicologia, Alma Mater Studiorum – Università di Bologna, Campus di Cesena, 47521 Cesena, Italy
Twitter Handle: @VincenzoRomei

Summary

It is commonly held that what we see and what we believe we see are overlapping phenomena. However, dissociations between sensory events and their subjective interpretation occur in the general population and in clinical disorders, raising the question as to whether perceptual accuracy and its subjective interpretation represent mechanistically dissociable events. Here, we uncover the role that alpha oscillations play in shaping these two indices of human conscious experience. We used electroencephalography (EEG) to measure occipital alpha oscillations during a visual detection task, which were then entrained using rhythmic-TMS. We found that controlling pre-stimulus alpha-frequency by rhythmic-TMS modulated perceptual accuracy but not subjective confidence in it, while controlling post-stimulus (but not pre-stimulus) alpha-amplitude modulated how well subjective confidence judgments can distinguish between correct and incorrect decision, but not accuracy.

These findings provide the first causal evidence of a double-dissociation between alpha-speed and -amplitude, linking alpha-frequency to spatio-temporal sampling resources, and alpha-amplitude to the internal, subjective representation and interpretation of sensory events.

Keywords: Conscious Perception, Alpha Oscillations, Alpha Amplitude, Alpha Frequency, Visual Perception, Confidence, Rhythmic Transcranial Magnetic Stimulation, Alpha Entrainment.

Introduction

The well-known axiom “Seeing is believing” implies that what we see and what we *believe* we see are largely overlapping phenomena. However, there are many examples of dissociations between sensory events and their subjective interpretation, both in the general population (i.e. false memories[1,2]) and in subclinical[3,4] and clinical psychiatric populations (e.g. schizophrenia[5]). A key question, therefore, is whether perceptual accuracy and its subjective interpretation represent mechanistically dissociable events of our conscious experience. And, if so, what their neural underpinnings might be.

Alpha oscillations (range 7-13Hz) in the human brain may play an active role in both sensory processing and conscious perception[6–15]. In particular, pre-stimulus alpha-amplitude has been shown to account for a momentary level of cortical excitability[16] and to predict subjective confidence in response to visual stimuli[17–19]. Specifically, higher levels of alpha-amplitude seem to account for reduced subjective confidence and reduced proneness to reporting a visual percept (more conservative decision criterion), without affecting the level of accuracy of the response[20]. These new insights into the role of alpha-amplitude in perception suggest that alpha-amplitude might not primarily reflect perceptual accuracy, but rather a change in the internal response criterion. However, this leaves open a fundamental question: what are the oscillatory correlates of perceptual accuracy?

Recent reports have highlighted the relevance of alpha-frequency in perceptual sampling, with faster alpha oscillations resulting in higher temporal resolution and more accurate perceptual experience[21–27], potentially through an increased accumulation of sensory evidence over time. Importantly, we hypothesize here that this higher temporal resolution of visual sampling can successfully translate into higher accuracy in general, by allocating more resources to the perceptually relevant sensory dimension within the same amount of time.

Here, in a first experiment, we have used a visual detection task with spatially lateralized stimuli and electroencephalography (EEG), to directly test the hypotheses that (1) alpha-frequency accounts for objective accuracy (correct vs. erroneous responses and d' measures[28]), while (2) alpha-amplitude predicts subjective confidence (low vs. high confidence responses) and/or (3) relates to meta-cognitive abilities, i.e. how well subjective confidence judgments can distinguish between correct and incorrect decisions (as indexed by meta-d' measures[29]).

Crucially, in a second experiment, we used rhythmic Transcranial Magnetic Stimulation (rhythmic-TMS) prior to stimulus onset around individual alpha-frequency (IAF) to entrain pre-stimulus oscillatory activity in the alpha-band towards slower or faster alpha-frequency or higher alpha-amplitudes, in order to influence individual performance towards lower or higher accuracy or to impact individual subjective confidence levels, respectively.

Finally, as stimulus processing has been shown to influence metacognitive abilities[30–32], in a third experiment, we delivered rhythmic-TMS at each participant's own IAF post-stimulus but prior to a subjective confidence prompt to test how increases in post-stimulus alpha-amplitude can modulate their ability to distinguish between correct and incorrect decisions, measured by means of meta-d'.

Results

A total of 92 participants took part in three experiments (Figure 1), designed to map pre-stimulus alpha-frequency and alpha-amplitude on objective versus subjective performance measures (EEG Experiment 1) and to test for their causative relationships (TMS-EEG Experiments 2&3).

Alpha-frequency and alpha-amplitude dissociate with respect to objective accuracy, subjective confidence and metacognitive abilities

In Experiment 1, twenty-four participants (12 women; mean age=23.2, SE=2.61) performed a visual detection task (Figure 1A) in which lateralized stimuli (8X8 checkerboards) were preceded by a spatially uninformative cue (an X), indicating that a stimulus will be occurring in the lower left- or right-hemifield with 50% probability (chance level). Each black and white checkerboard was flashed for 60ms and could contain iso-luminant grey circles, the contrast of which was set for each individual to their 50% perceptual threshold. Half of the trials were catch trials, i.e. checkerboards without any grey circle embedded in them (see Methods for details).

Participants were instructed to respond whenever they perceived grey circles within the lateralized checkerboards. Following this primary task and about 1.5-2sec post-stimulus, they were prompted to indicate on a scale of 1 to 4 how confident they were of their percept, with 1 representing “no confidence at all”, 2, “little confidence”, 3 “moderate confidence” and 4 “high confidence” (see Figure 1A). EEG signals were concurrently recorded from 64 electrodes while this task was performed (see Methods).

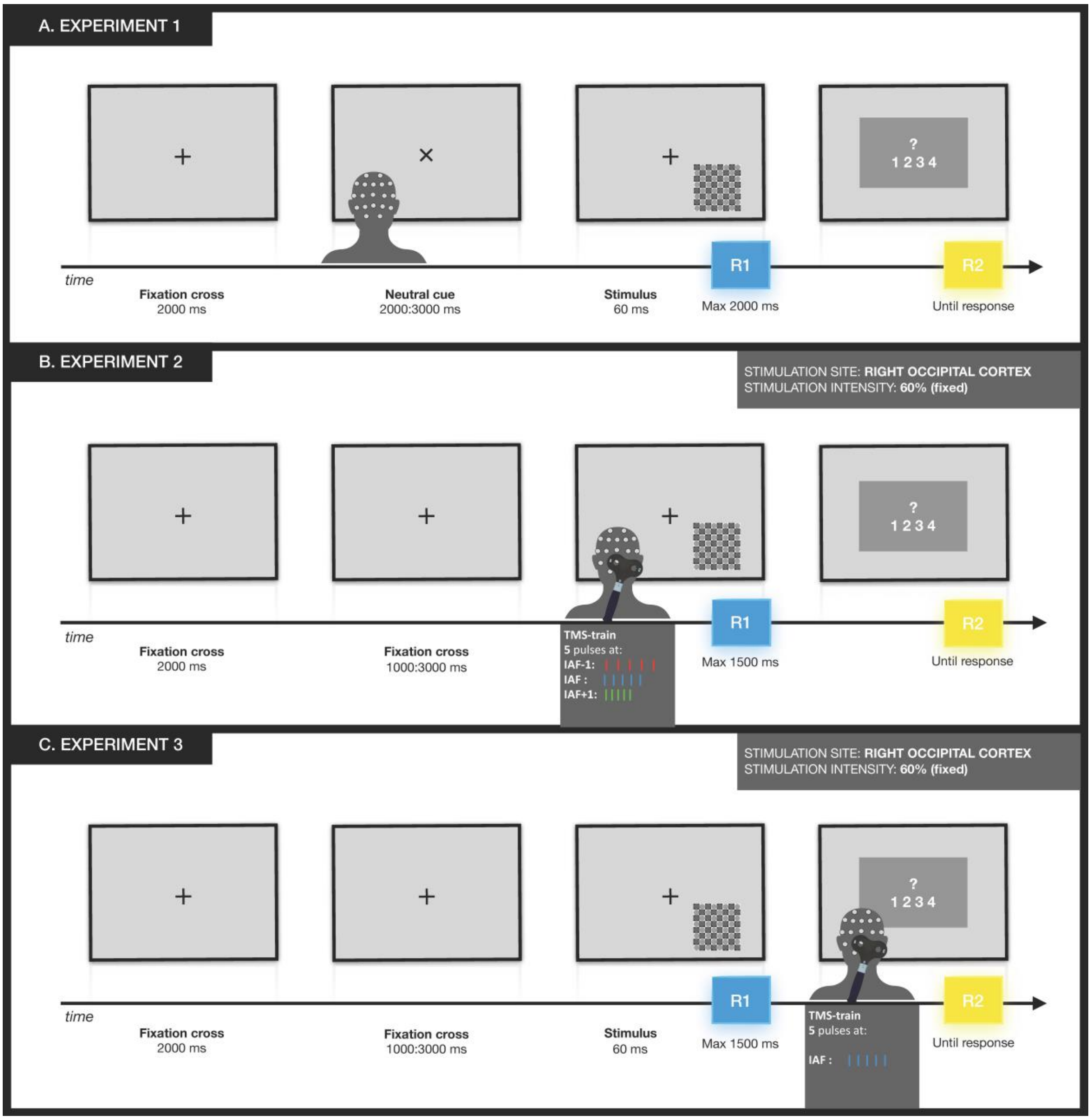

Figure 1. Experimental design. A. Experiment 1: EEG data were collected during a visual detection task. Each trial started with a fixation cross, after which stimuli could randomly appear in the lower left or right visual field. The primary task was to respond (R1) by pressing a space bar if the checkerboard contained grey circles. After this, participants rated their confidence in their first response (R2) on a Likert scale from 1 (no confidence at all) to 4 (high confidence). B. Experiment 2: Participants performed the same visual detection task as in Experiment 1 while undergoing concurrent EEG recording. In addition, 5 rhythmic-TMS pulses were administered before stimulus presentation. Participants were assigned to 3 different groups. For each group, rhythmic-TMS pulses were set at a certain alpha-frequency: individual alpha-frequency (IAF) group (blues bars), slower pace (IAF-1Hz) group (red bars), and faster pace (IAF+1Hz) group (green bars). C. Experiment 3: Participants performed the same visual detection task while undergoing EEG recordings, as in Experiments 1 and 2. However, rhythmic-TMS pulses were administered before the confidence prompt at each participant's individual alpha-frequency. ms=milliseconds.

Pre-stimulus alpha-frequency and accuracy: We looked at whether correct vs. erroneous responses could be best explained by the frequency of alpha oscillations prior to stimulus presentation, rather than by their amplitude. Our analysis of pre-stimulus alpha-frequency (Figure 2A) showed a significant main effect of ACCURACY (Correct vs. Errors) ($F(1,23)=18.2$, $p<.001$, $\eta_p^2=.442$). This result suggests that individual pre-stimulus alpha-frequency can differentiate between correct and erroneous responses, with faster alpha-frequency predicting correct responses (M=11.45Hz, SE=0.18Hz) and slower alpha-frequency predicting errors (M=11.02Hz, SE=0.18 Hz). Moreover, the effect of alpha-frequency was maximal over the posterior electrodes (Figure 2A, map inset), involving left and right sites equally, as no main effect of HEMISPHERE (ipsilateral vs. contralateral to the presented stimulus) ($F(1,23)=1.34$, $p=.259$, $\eta_p^2=.06$), nor a significant interaction of ACCURACYxHEMISPHERE ($F(1,23)=0.33$, $p=.571$, $\eta_p^2=.014$) were found.

We further tested whether pre-stimulus alpha-frequency can predict individual performance across participants as assessed by d’, a sensitivity index that takes into account both correct responses and false alarms, and thus – relative to the simple hit rate measure – has the advantage of discounting any potential effect of response bias, with higher values reflecting higher task accuracy[28]. Using a median split procedure for d’ scores, we divided participants in two numerically equivalent groups (high vs low d’). In line with our hypothesis, a between-groups analysis of alpha-frequency show faster pre-stimulus alpha-frequency in the high d’ group (11.55Hz, SE=0.22Hz) compared to the low d’ group (10.29Hz, SE=0.66Hz) by 1.26Hz: $t(22)=1.832$, $p=.040$, $d=.374$ (one-tailed unpaired two-sample t-test).

By contrast, the analysis of both pre- and post-stimulus alpha-amplitude (see supplemental Figure S1B) showed no significant effects on ACCURACY (*all Fs* (1,23)<3.05, *all ps*>.094, *all* ηp^2<.117), in line with recent reports that alpha-amplitude does not account for objective accuracy[9,17,18,33].

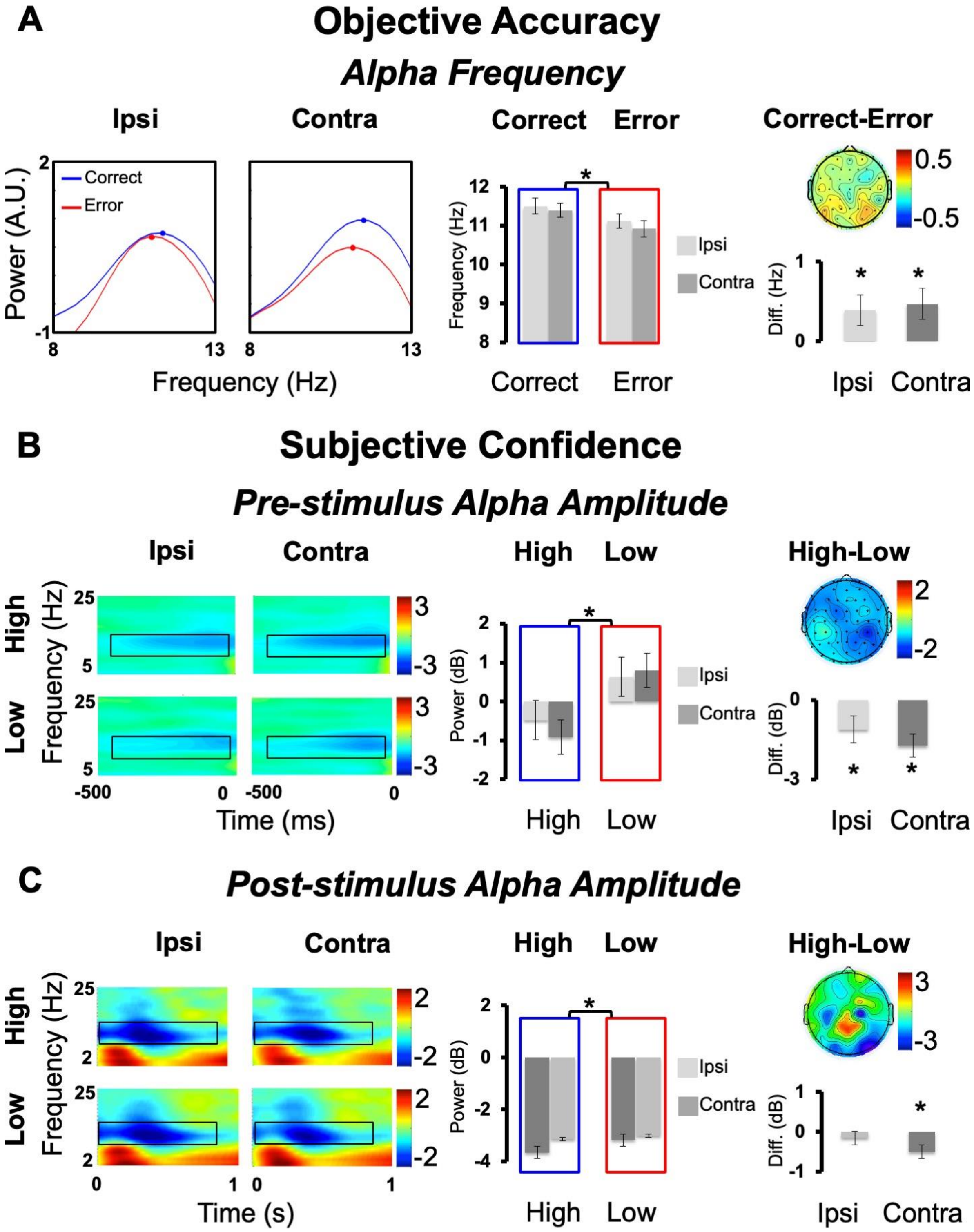

Figure 2. Results Experiment 1: Alpha-frequency and -amplitude relate to accuracy and confidence. A. Objective Accuracy. Averaged *alpha-frequency* is represented as the z-scored mean power ($10*\log_{10}[\mu v^2/Hz]$) spectrum in the cue-stimulus time period for the contralateral and the ipsilateral electrodes and for Correct and Error trials within the alpha-band. Bar graphs report correct and error trials and the differences in correct/error responses. Topography represents the difference in Correct-Error (electrodes are flipped to represent contralateral activity in the right-hand side and ipsilateral activity in the left-hand side). Subjective Confidence. Pre-stimulus alpha-amplitude (B) and post-stimulus alpha-amplitude (C) are reported as time-frequency plots. For illustrative purposes we reported data from a cluster of ipsi (P7,PO7,PO3,O1) and contralateral (P8,PO8,PO4,O2) electrodes and for Low and High confident trials. Black boxes denote regions of statistical analyses (alpha-band 7-13Hz). Bar graphs are reported for Low and High confident trials and for the difference in High-Low. Topography represents the difference in High-Low (electrodes are flipped to have contralateral activity in the right-hand side and ipsilateral activity in the left-hand side). Two-tailed t-test statistical significance is reported (*p<.05). Error bars represent standard error of the mean. A.U.=arbitrary units; Diff=difference; μv=microvolt; Hz=Hertz; ms=milliseconds; dB=decibel. See also Figure S1.

Pre-stimulus alpha-amplitude and confidence: We then tested whether pre-stimulus alpha-amplitude, rather than alpha-frequency, could account for confidence judgments[17,18,6] (Figure 2B). We found a main effect of CONFIDENCE ($F(1,23)=9.03$, $p=.006$, $\eta_p^2=.282$), with desynchronized alpha-amplitude in high confidence trials (-0.699dB, SE=0.409dB) and synchronized alpha-amplitude in low confidence trials (0.719dB, SE=0.251dB), suggesting that alpha-amplitude has a significant impact on perceptual confidence. Moreover, topography (Figure 2B, map inset) shows posterior alpha-amplitude modulations with an even distribution across hemispheres, indicating no main effect of HEMISPHERE (ipsilateral vs. contralateral to the presented stimulus) $F(1,23)=0.201$, $p=.658$, $\eta_p^2=.009$), nor a significant interaction CONFIDENCExHEMISPHERE ($F(1,23)=1.323$, $p=.262$, $\eta_p^2=.054$).

For completeness, control analyses performed on pre-stimulus alpha-frequency (see supplemental Figure S1A) showed no main effect of CONFIDENCE, nor any interaction with HEMISPHERE (all $Fs(1,23)<0.47$, $ps>.501$, $\eta_p^2<.021$).

Post-stimulus alpha-amplitude, confidence and meta-d': Because following stimulus presentation the initial choice on decisions and confidence continue to evolve[31,32], we asked whether subjective confidence judgments are influenced by post-perceptual processes. To this aim, we analysed alpha-amplitude in a time window after stimulus presentation (0-900ms), corresponding to a post-stimulus time period but before the confidence prompt (Figure 2C). The analysis of post-stimulus alpha-amplitude revealed a main effect of CONFIDENCE ($F(1,23)=4.367$, $p=.048$; $\eta_p^2=.16$), with more desynchronized alpha-amplitude in high confidence trials (-3.41dB, SE=0.38dB) compared to low confidence trials (-3.08db, SE=0.34dB). Moreover, the analyses showed a main effect of HEMISPHERE ($F(1,23)=5.358$; $p=.03$; $\eta_p^2=.189$) and most importantly, an interaction CONFIDENCExHEMISPHERE ($F(1,23)=4.347$, $p=.048$, $\eta_p^2=.159$), showing that when looking at post-stimulus alpha-amplitude, the confidence effects are accounted for by the contralateral (high confidence=-3.64dB, SE=0.396dB; low confidence=-3.14dB, SE=0.347dB; $t(23)=2.747$, $p=.011$; $d=.586$) but not the ipsilateral hemisphere (high confidence=-3.17dB, SE=0.387dB; low confidence=-3.01dB, SE=0.349dB; $t(23)=0.906$, $p=.375$, $d=.193$). These findings suggest that post-stimulus alpha-amplitude has a retinotopic distribution being modulated by the stimulus position. Indeed, while the relationship between confidence levels and pre-stimulus alpha-amplitude can be observed for both hemispheres, only contralateral alpha-amplitude accounts for individual confidence levels after stimulus presentation.

We then tested whether post-stimulus alpha-amplitude could specifically account for metacognitive abilities. In other words, we tested how well subjective confidence judgments can distinguish between correct and incorrect decisions, by means of meta-d', a measure that quantifies metacognitive performance and that reflects the efficacy of confidence ratings to discriminate objectively correct from erroneous responses[29]. In a between-subject design, by using a median-split procedure, we divided participants with high and low metacognitive abilities. We found that post-stimulus alpha-amplitude in the high meta-d’ group was significantly more desynchronized (-4.66dB, SE=0.59dB) relative to the low meta-d’ group (-3.26dB, SE=0.39dB; one-tailed unpaired two-sample t-test: *t*(22)=1.966, *p*=.031; *d*=.567), thus supporting the idea that post-stimulus alpha-amplitude can predict metacognitive performance. Moreover, this role seems specific for post-stimulus alpha-amplitude, as pre-stimulus changes of alpha-amplitude could not account for between-subject differences in metacognition (*t(*22)=0.929, *p*=.181, *d*=.189), further supporting this interpretation.

Overall, these EEG results implicate alpha-frequency in the level of objective accuracy with higher alpha-frequency accounting for higher accuracy, but playing no role in determining one’s individual perceptual confidence. Conversely, alpha-amplitude is implicated in perceptual decision confidence, but has no role to play in objective accuracy. In sum, these results point to a functional dissociation of the two oscillatory markers, alpha-frequency and alpha-amplitude, which appear to shape sensory sampling and the subjective readout of this sampling, respectively.

Entraining faster vs. slower pre-stimulus alpha oscillations selectively shapes objective accuracy

In Experiment 2, we tested for the causal involvement of alpha-frequency and alpha-amplitude in objective accuracy vs. confidence by using rhythmic-TMS to entrain alpha oscillations while participants performed the same visual task as in

Experiment 1 (Figure 1B). In three different experimental groups (N=3x17 participants; 25 women; mean age=23.39, SE=0.36), we recorded EEG activity while concurrently administering 5-pulse rhythmic-TMS trains of fixed-intensity (60% of the maximum stimulator output)[34,35] to the right occipital cortex (coil placement over O2) prior to stimulus presentation. In the IAF±1Hz groups, rhythmic-TMS-frequency was set at 1Hz faster/slower than the individual participant's alpha-frequency, which should entrain their alpha oscillations towards a faster/slower pace[21,22,36], respectively. In the IAF group, the rhythmic-TMS frequency was aligned with the participant's alpha-frequency. This has been shown to lead to enhanced alpha-amplitude by entrainment[37,38], and should thus have an impact on confidence rather than on accuracy. Together with active rhythmic-TMS, we employed sham stimulation at a matching frequency for every participant in each group, to account for any nonspecific effects of rhythmic-TMS.

Perceptual accuracy was quantified via d' score[28] (shown to be a more sensitive measure relative to hit rates) while task confidence was estimated via mean confidence and meta-d'. All measures were analysed across the two hemifields (left vs. right), the two stimulation types (active rhythmic-TMS vs. sham), and the three groups of participants (stimulated at IAF±1Hz and IAF).

We looked at the impact of rhythmic-TMS on EEG activity across the 3 groups (Figure 3). As expected, pre-stimulus alpha-frequency was modulated differently in active rhythmic-TMS versus sham stimulation across the experimental groups, depending on the recording site (STIMULATIONxGROUPxHEMISPHERE interaction: $F(2,48)=4.05$, $p=.024$, $\eta_p^2=.144$). Specifically, stimulating at the lower alpha-frequency slowed down pre-stimulus alpha activity during active rhythmic-TMS (M=9.74Hz, SE=0.20), relative to sham stimulation (M=10.66Hz, SE=0.20), selectively at the (stimulated) right hemisphere (*t*(16)=3.98, *p*=.001, *d*=.96). Conversely, stimulation at the higher alpha-frequency led to faster pre-stimulus alpha activity during active rhythmic-TMS (M=11.11Hz, SE=0.14), relative to sham stimulation (M=10.43Hz, SE=0.31), selectively at the stimulated site (*t*(16)=2.19, *p*=.043, *d*=.53). Finally, stimulation at the exact alpha-frequency did not yield any difference in the pre-stimulus alpha speed (*t*(16)=0.13, *p*=.90, *d*=.03). Moreover, we found that rhythmic-TMS maximally entrained oscillatory activity exactly at the site of stimulation (HEMISPHERExSTIMULATION interaction: *F*(1,48)=6.36, *p*=.015, η_p^2=.117), and at the entrained rhythm (see Figure 3A).

By contrast, the broadband alpha-amplitude (see Figure 3B) did not differ significantly across the three groups during the entrainment protocol (HEMISPHERExSTIMULATIONxGROUP interaction: *F*(2,48)=0.19, *p*=.830, η_p^2=.008). However, the entrainment effect on alpha-amplitude (quantified via the difference between active rhythmic-TMS and sham stimulation) was largest at the frequency of stimulation (FREQUENCYxGROUP interaction: *F*(4,96)=5.640, *p*<.001, η_p^2=.19, for details, see supplemental figure S2).

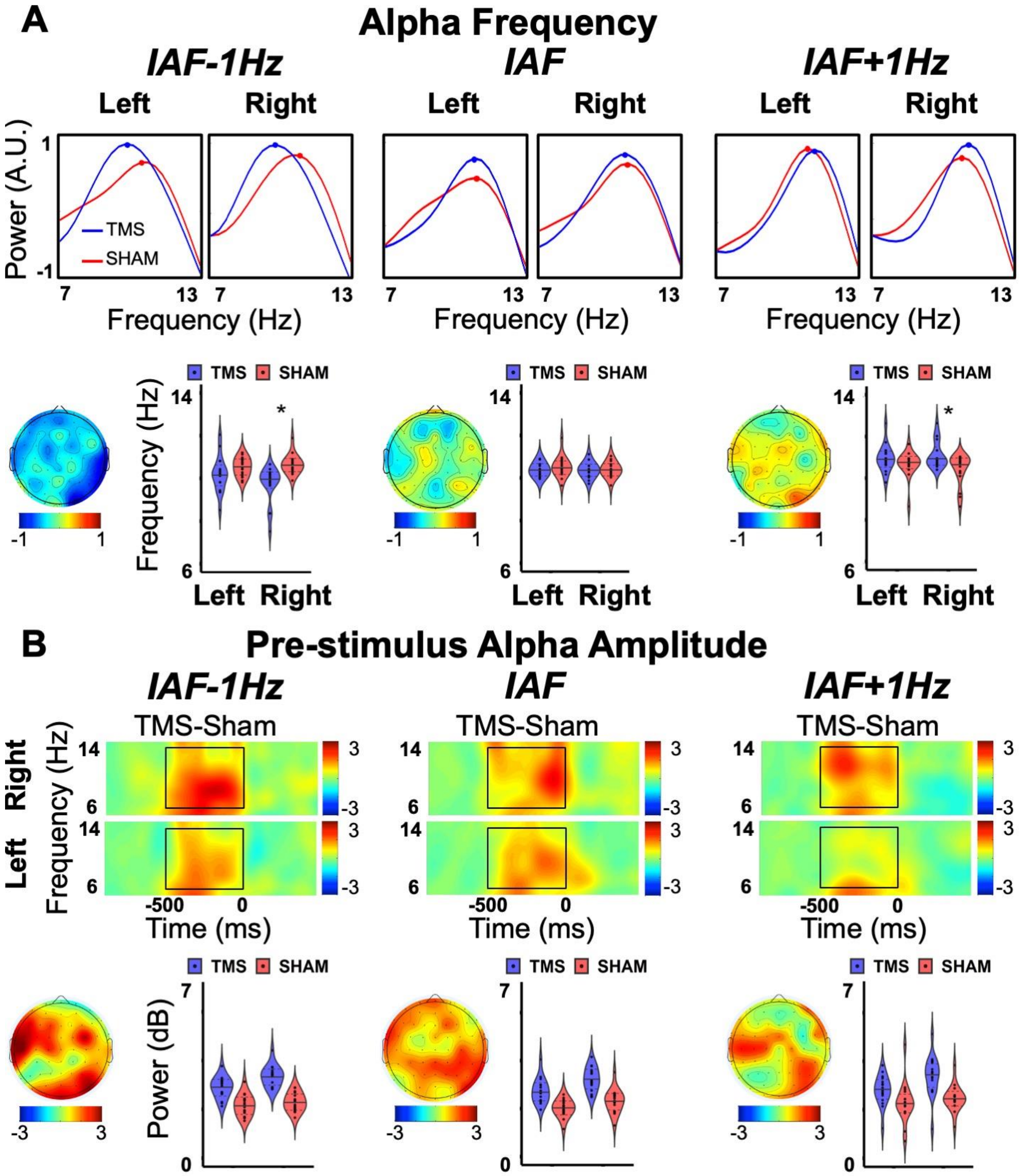

Figure 3. Results Experiment 2: rhythmic-TMS entrainment modulates EEG alpha-frequency and its amplitude. Results are shown for each group performing the task in Experiment 2 under different rhythmic-TMS alpha entrainment protocols (IAF±1Hz, IAF). A. (Upper) Averaged Alpha-frequency is represented as the z-scored mean power ($10*\log_{10}[\mu v^2/Hz]$) spectrum during rhythmic-TMS in the pre-stimulus time period (-650 0) in the right (stimulated) hemisphere (electrode cluster: O2,PO4,PO8) and left (non-stimulated) hemisphere (electrode cluster: O1,PO3,PO7), for active rhythmic-TMS (TMS) and SHAM-control stimulation. (Lower) Violin plots report peak frequency during TMS and SHAM for each group (IAF±1Hz, IAF) and for the left and right (stimulated) hemisphere. Data are

presented as median (full line) ±1 quartile (dashed line). The topography image represents the difference in alpha-frequency between TMS and SHAM stimulation. B. (Upper) Pre-stimulus alpha-amplitude is presented as time-frequency plots for each group (IAF±1Hz, IAF) of the difference between TMS and SHAM stimulation in the right (stimulated) hemisphere (electrode cluster: O2,PO4,PO8) and in the left (non-stimulated) hemisphere (electrode cluster: O1,PO3,PO7). Black boxes denote regions of statistical analyses (alpha-band 7-13Hz in the pre-stimulus period (-500,0)). (Lower) Violin plots report alpha power during TMS and SHAM for each group, and for the left and right (stimulated) hemisphere. Data are presented as median (full line) ±1 quartile (dashed line). Topography represents the difference in alpha-amplitude between TMS and SHAM stimulation. Two-tailed t-test statistical significance is reported (*p<.05). Error bars represent standard error of the mean. A.U.=arbitrary units; Diff=difference; μv=microvolt; Hz=Hertz; ms=milliseconds; dB=decibel.

When examining the impact of entrainment on behavior (Figure 4A), we found that speeding up or slowing down alpha oscillations had a direct impact on performance (STIMULATIONxGROUPxHEMIFIELD interaction ($F(1,48)=3.25$, $p=.047$, $\eta p^2=.119$). Specifically, slowing-down pre-stimulus alpha-frequency led to lower d’ scores in the active rhythmic-TMS condition (relative to sham stimulation) exclusively in the hemifield contralateral to stimulation ($t(16)=2.67$, $p=.017$, $d=.65$). In contrast, speeding-up pre-stimulus alpha-frequency led to higher d’ values during active rhythmic-TMS (relative to sham stimulation), exclusively in the contralateral hemifield ($t(16)=2.52$, $p=.023$, $d=.61$). Finally, entrainment at individual alpha-frequencies did not yield differences in task accuracy, as predicted (all ts(16)<1.19, all ps>.252, all ds<.29). We further tested whether the impact of rhythmic-TMS on EEG oscillatory activity could account for the magnitude of the behavioral modulation induced by the TMS protocol (Figure 4B). To do so, we examined the relationship between sham-corrected performance and sham-corrected entrained frequency across participants (IAF±1Hz groups included). The results reveal that a significant positive relationship exists between the TMS-induced change in oscillatory peak frequency and performance gain (R^2=0.29, p=.001), further confirming a link between alpha-frequency and performance accuracy.

Our results thus far indicate that pre-stimulus alpha-frequency, but not alpha-amplitude, has a causative role in sampling sensory input, accounting for visual accuracy.

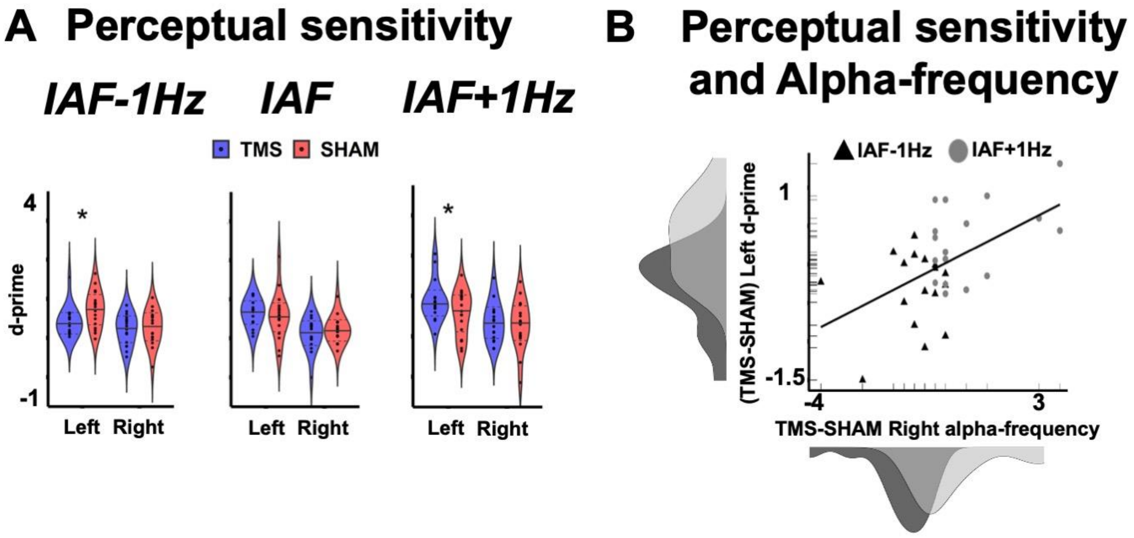

Figure 4. Results Experiment 2: rhythmic-TMS entrainment causally links alpha speed to perceptual accuracy. A. Perceptual sensitivity. Results are presented for three groups of participants (IAF±1Hz and IAF stimulation protocol). Perceptual sensitivity is quantified in d' scores. Violin plots of d' are reported for rhythmic-TMS (TMS) and SHAM-control stimulation, and separately for the left and right hemifields. Data are presented as median (full line) ±1 quartile (dashed line). B. Perceptual sensitivity and alpha-frequency. Relationship between TMS-induced differences in alpha-frequency in the stimulated (right) hemisphere (computed as a difference in alpha-frequency between TMS and SHAM stimulation) and differences in accuracy in the opposite (left) hemifield (computed as a difference in d' score between TMS and SHAM stimulation), across the slower (IAF-1Hz group, represented as black triangles) and faster rhythmic-TMS groups (IAF+1Hz group, represented as grey circles). Density distributions of the two variables across the two groups are also presented along the corresponding axes. t-test statistical significance is reported (*p<.05).

Alpha-amplitude dynamics shape subjective confidence and metacognition, not accuracy

Another goal of Experiment 2 was to determine whether alpha-amplitude dynamics causally shape subjective representation and interpretation of perceptual performance. However, confidence levels and metacognitive abilities – as measured via confidence mean and meta-d' scores[29] respectively – appeared not to be affected across the three different stimulation protocols nor between the two hemifields, as neither the main effects of GROUP, HEMIFIELD and STIMULATION, nor their interactions, reached significance (all Fs(2,48)< 2.72, all ps>.076, all ηp^2<.102). The short-term nature of entrainment effects might explain these null results, as they are limited to a few hundreds of milliseconds following stimulation[37,39,40]. This is long enough for pre-stimulus TMS entrainment to influence the primary accuracy response, as this was collected immediately after stimulus presentation. The secondary, higher decision confidence response, however, which was associated with pre-stimulus EEG alpha-amplitude, was collected only 1.5-2 sec post-stimulus (through the confidence prompt) and hence occurred >1 sec after rhythmic-TMS offset (see Figure 1B), when entrainment effects might not be sufficiently sustained anymore[37,41]. Therefore, in order to further assess the causal role of alpha-amplitude dynamics in perceptual awareness, and particularly in metacognitive abilities, we ran a third follow-up experiment aimed at entraining post-stimulus alpha-amplitude in seventeen participants (12 women; mean age=22.47, SE=0.66). This group received 5-pulse rhythmic-TMS trains that were tailored to their individual alpha-frequency with pulses applied just before the confidence prompt, i.e. after stimulus presentation (see Figure 1C). The aim of this protocol was to enhance alpha-amplitude by rhythmic-TMS without affecting alpha-speed. Importantly, analysis of the alpha-amplitude in the post-stimulus period in Experiment 1 justified the timing of this stimulation, as alpha-amplitude after stimulus presentation (i.e. the time window of stimulation in Experiment 3) was related to subjective confidence (with lower contralateral alpha-amplitude leading to high confidence responses) and metacognitive abilities.

EEG analyses in Experiment 3 revealed a maximal entrainment effect in broadband alpha-amplitude prior to the confidence prompt during active rhythmic-TMS relative to sham stimulation at the stimulated site (HEMISPHERExSTIMULATION interaction: $F(1,16)=6.91$, $p=.002$, $\eta p^2=.302$). Moreover, as expected, the rhythmic-TMS trains at IAF did not have any effect on the alpha frequency measured prior to confidence judgment (all $Fs(1,16)< 0.19$, all $ps>.666$, all $\eta p^2<.012$) (Figure 5A, B). Crucially, this selective modulation of alpha-amplitude right before confidence judgment allowed us to causally test the impact of alpha-amplitude on metacognitive abilities vs. subjective confidence ratings. Our results show clear effects on metacognition, as highlighted by distinct modulations of meta-d’ scores, between active rhythmic-TMS and sham stimulation, depending on hemifield (HEMIFIELDxSTIMULATION interaction: $F(1,16)=4.73$, $p=.045$, $\eta p^2=.228$) (Figure 5C). Specifically, higher alpha-amplitudes prior to the confidence prompt led to lower meta-d’ scores during active rhythmic-TMS vs. sham stimulation, exclusively in the contralateral hemifield ($t(16)=2.74$, $p=.014$, $d=.66$). Importantly, these induced changes in post-stimulus alpha-amplitude had a selective impact on metacognitive abilities and not on confidence measures or on perceptual accuracy (*all* $Fs(1,16)<.82$, *all* $ps>.379$, all $\eta_p^2<.049$), thus confirming the role of post-stimulus alpha-amplitude in higher-level post-perceptual decision making.

Finally, we tested whether individual differences in TMS-induced post-stimulus alpha-amplitude modulations could account for the level of metacognitive abilities. To do so, we analyzed the relationship between sham-controlled TMS-induced alpha-amplitude and sham-controlled meta-d’ levels for stimuli presented in the contralateral hemifield. We found a significant inverse relationship, confirming that the higher the impact of rhythmic-TMS on alpha-amplitude, the lower the resulting level of metacognition of the individual response (*R^2*=0.27, *p*=.032; *Fig*ure 5D). These results strongly support a role of post-stimulus alpha-amplitude in selectively shaping our metacognitive abilities, with higher post-stimulus alpha-amplitude leading to lower metacognition.

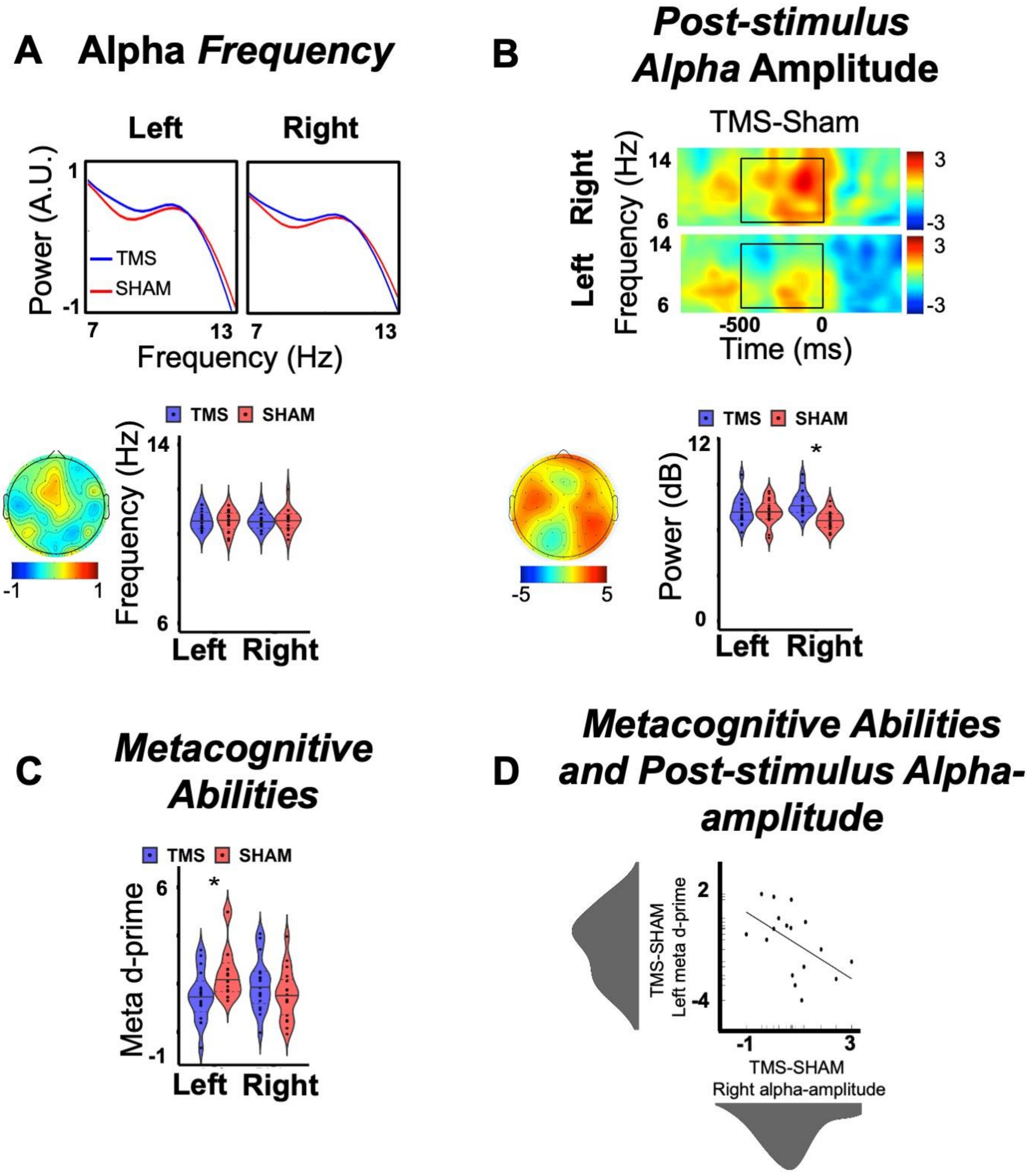

Figure 5. Results Experiment 3: rhythmic-TMS entrainment causally links post-stimulus alpha-amplitude to metacognitive abilities. A. (Upper) Averaged Alpha-frequency is represented as the z-scored mean power ($10*\log_{10}[\mu v^2/Hz]$) spectrum in a pre-confidence time period (850 1500) in the right (stimulated) hemisphere (electrode cluster: O2,PO4,PO8) and in the left (non-stimulated) hemisphere (electrode cluster: O1,PO3,PO7) for rhythmic-TMS and SHAM-control stimulation. (Lower) Violin plots report peak frequency during TMS and SHAM, separately for the left and right (stimulated) hemisphere. Data are presented as median (full line) ±1 quartile (dashed line); Topography represents the difference in alpha-frequency between TMS and SHAM stimulation. B. (Upper) Post-stimulus alpha-amplitude reported as a time-frequency plot of the difference between TMS and SHAM stimulation in the right (stimulated) hemisphere (electrode cluster: O2,PO4,PO8) and in the left (non-stimulated) hemisphere (electrode cluster: O1,PO3,PO7). Black boxes denote regions of statistical analyses (alpha-band 7-13Hz in the pre-confidence stimulation period (1000,1500)). (Lower) Violin plots report alpha-power during TMS and SHAM stimulation, and separately for the left and right (stimulated) hemisphere. Data are presented as median (full line) ±1 quartile (dashed line). Topography represents the difference in alpha-amplitude between TMS and SHAM stimulation. C. Metacognitive Abilities, quantified via meta-d’ scores. Violin plots of meta d’ for TMS and SHAM-control stimulation, and reported separately for the left and right hemifields. Data are presented as median (full line) ±1 quartile (dashed line). D. Metacognitive Abilities and Post-stimulus Alpha-amplitude. Relationship between rhythmic-TMS-evoked differences in alpha-amplitude in the stimulated (right) hemisphere (computed as a difference in alpha-amplitude between TMS and SHAM stimulation) and differences in metacognition in the opposite (left) hemispace (computed as a difference in meta-d’ score between TMS and SHAM stimulation). Density distributions of the two variables are also presented along the corresponding axes. Two-tailed t-test statistical significance is reported (*p<.05). A.U.=arbitrary units; μv=microvolt; Hz=Hertz; ms=milliseconds; dB=decibel.

Discussion

The oscillatory underpinnings of conscious perception have been the focus of many studies, yet they remain largely unknown. A number of studies have previously reported that pre-stimulus alpha oscillations over occipital sites might play a role in human perceptual performance prediction[e.g.16,42–45], highlighting the potential existence of a direct link between levels of alpha activity, cortical excitability and perceptual sensitivity. Recent findings[17,18,20,33,46] have, however, challenged these past interpretations, and have highlighted the need to dissociate the processes that shape perceptual sensitivity from those that shape the subjective interpretation of a sensory event[28]. Here, we disentangle the oscillatory dynamics of these two processes and go beyond a correlative approach. By using an information-based rhythmic-TMS protocol[36], we demonstrate that distinct markers of alpha activity have a causal role in shaping our conscious perception, a role that goes beyond that of a simple epiphenomenon. By directly manipulating alpha-frequency and -amplitude at the site of stimulation[47,48], we were able to dissociate perceptual sensitivity from the subjective representation and interpretation of a sensory event, thus demonstrating their dualistic nature.

Our findings show that the speed of occipital alpha activity has a crucial and selective role in modulating perceptual sensitivity. This adds to previous reports showing that alpha cycles account for sampling sensory information into discrete units/perceptual frames (initially proposed by[49] and reviewed in[12]). From this, one might expect that higher frequency would translate in higher accuracy when information can be sampled over many cycles. But why would this effect show even when a sensibly short-lasting stimulus, certainly shorter than one alpha cycle, is presented, as in our case? With our experimental design (60ms stimulus duration), there is only one chance (sample) to capture the stimulus within an alpha cycle. And what would this tell us about the underlying mechanism? To address this, we provide here an exemplar account of the impact of frequency variations on sampling efficacy for a 9Hz and 11Hz alpha oscillation. For these oscillations, cycles will range between 110ms (for 9Hz IAF) and 90ms (for 11Hz IAF). However, processing abilities will vary within the cycle, with a rapid fluctuation from a high to low excitability phase (from alpha peak to through)[50–53]. Hence, sampling is expected to occur in one half of this cycle only, i.e. during ~55ms for 9Hz and ~45ms for 11Hz, respectively. Our data suggest that this sampling is more effective with higher than lower alpha frequencies, even with stimuli as short as 60ms, suggesting that evidence accumulation already starts to differ within one sampling sweep across variations of alpha-frequencies. This can be explained by enhanced processing capacities for shorter than longer cycles, because with the shorter sampling phases (~45ms), our short-lasting stimulus (60ms) is more likely to be fully comprehended in one perceptual frame. For stimuli of longer durations (e.g. 1000ms), one would expect repeated sampling sweeps to further add to this difference, as more full-sample sweeps can be packed in 1sec at high than low frequencies (11 vs. 9 sweeps, for 11Hz vs 9Hz). In sum, here we claim that in line with existing literature[23,24,33] higher frequencies are expected to aid temporal resolution by creating more sampling frames per second; but our data show that, at the same time, in the context of our specific experiment, higher frequency also means that less time is employed to create a single sampling frame, leading to higher processing capacities.

Our EEG findings furthermore show an inverse relationship between levels of alpha-amplitude and subjective confidence confirming previous findings[17–19]. Indeed, pre-stimulus alpha-amplitude has been proposed to relate to internal decision-making variables[18,20], rather than perceptual accuracy per se. Yet, our experimental manipulation by rhythmic-TMS could not verify the existence of a causal link between pre-stimulus alpha-amplitude and confidence. However, several studies have concluded that our sense of confidence is also determined by processes that occur after we make a choice, thus integrating sensory evidence and improving our “metacognitive accuracy”, namely the extent to which our confidence is consistent with our probability of being correct[e.g.31,54,55]. Examining post-stimulus alpha-amplitude, Experiments 1 and 3 demonstrate that after lateralized stimuli are presented, perceptually relevant, post-stimulus alpha-amplitude become focused in the hemisphere contralateral to stimulus presentation, with lower alpha-amplitude leading to higher perceptual confidence. Moreover, these levels of post-stimulus alpha desynchronization directly account for metacognitive abilities across participants and can be causally manipulated by rhythmic-TMS. These latter results suggest that post-stimulus alpha modulations may reflect the integration of confidence judgment with the accumulated evidence after stimulus presentation to update and adjust metacognitive decisions[31,55,56]. Taken together, these results speak in favor of a relevant role of alpha-amplitude in post-perceptual decision making. Therefore, it might be possible that pre-stimulus alpha-amplitude dictates the initial level of perceptual bias (effects observed for confidence bilaterally, but not metacognitive effects), that subsequently integrates sensory evidence brought by the stimulus itself (reflected in hemisphere-specific processes), resulting in post-perceptual estimation of the performance.

While our experiments show that alpha-frequency and –amplitude, and hence sensitivity and confidence, are dissociable entities, these processes likely work in concert in more ecological situations to maximize the efficiency of our conscious experience. We observed that the entrainment effects on oscillation and perception showed corresponding topographic/retinotopic distributions, with perception being exclusively modulated in the hemifield contralateral to the stimulated site, suggesting that the oscillatory substrates of effective sampling and subjective confidence could be oriented in space to optimize the allocation of attention resources. Therefore, under controlled conditions (for example by presenting informative cues[57] or in predictive contexts[52] that are associated with spatial priors), one might expect the spatially specific co-occurrence of alpha-frequency and -amplitude modulation that is contralateral to the to-be-attended or expected location[59,60]. Future research into the inter-dependency of these two circuits may shed new light on different neuropsychological phenomena. For example, the failure to integrate perceptual processes and their subjective interpretation might lead to altered cognitive experiences, such as confabulations or the formation of false representations and memories, with relevant implications for clinical and forensic neuropsychology. The failure to integrate perceptual processes and their subjective interpretation may also lead to conscious departure from sensory events in acute schizophrenia patients[61].

In conclusion, our results point to a functional dissociation between the accuracy of what we see and our interpretation of it. We reveal that the sampling of visual information and its subjective interpretation, which are strongly inter-dependent in everyday life, are dissociable in terms of neural mechanisms in oscillatory activity. Specifically, alpha-frequency and -amplitude reflect the activity of these two independent mechanisms that serve complementary functions. Alpha-frequency represents a spatial and temporal sampling mechanism[27,62–64] that shapes perceptual sensitivity. By contrast, alpha-amplitude dictates more liberal vs conservative choices in confidence judgments, further modulated with incoming sensory evidence, thus having post-perceptual effect on how these subjective confidence judgments can distinguish between correct and incorrect decisions[17,19]. How these mechanisms interact to give rise to an integrated (or not) sense of our perceptual environment, is yet to be addressed. However, we demonstrate that these oscillatory processes can be selectively modulated by non-invasive neurostimulation, offering a foundation to future translational neuroscience approaches and clinical applications.

Acknowledgments

FDG is supported by the Ministero della Salute (SG-2018-12367527); AA is supported by Fondazione del Monte di Bologna e Ravenna (339bis/2017), Bial Foundation (347/18) and Ministero dell’Istruzione, dell’Università e della Ricerca (2017N7WCLP); VR is supported by the Bial Foundation (204/18);

Author contributions

VR conceived the project; VR, FDG, JT, CR, AA, GT designed the experiment; VR, FDG, EM, PDL, JT, CR, Implemented the experiment; JT, EM, PDL and CR conducted the experiment; FDG and JT analysed data; FDG, JT and VR wrote the first draft of the paper. VR, FDG, EM, PDL, JT, CR, AA GT contributed to the final draft of the paper.

Declaration of Interests

The authors declare no competing interests.

STAR Methods

Resource availability

Lead contact. Further information and requests for resources and reagents should be directed to and will be fulfilled by the Lead Contact, Vincenzo Romei (vincenzo.romei@unibo.it).

Materials availability. See the Key resources table for information about resources. This study did not generate new unique reagents.

Data and code availability. The datasets generated during this study have been made publicly available through the Open Science Framework (https://osf.io/e4bnj/). Any additional information required to reanalyse the data reported in this paper is available from the lead contact upon request.

Experimental model and subject details

Experiment 1

Participants: Twenty-four healthy volunteers (12 women, 12 men; mean age= 23.2, SE=2.61) with normal or corrected vision participated in Experiment 1. Sample size was determined based on previous literature. Specifically, previous EEG studies on the role of pre-stimulus alpha in conscious perception considered a sample size between 10 and 26 participants[18,33,65,66]. In addition, post-hoc power analysis (G-power 3.1) revealed that, for all significant ANOVA effects in our study, values of Power (1-β err prob) are >0.95. All participants were recruited at the Centre for Studies and Research in Cognitive Neuroscience in Cesena, Italy. The study was conducted in accordance with the Declaration of Helsinki. All participants gave written informed consent to participate in the study, which was approved by the bioethics committee of the University of Bologna.

Experiment 2

Participants. Fifty-one healthy volunteers (25 females, 26 males; mean age ± SE = 23.39 ± 0.36 years) took part in Experiment 2. Sample size was determined based on previous literature. Specifically, previous TMS studies on oscillatory entrainment considered a sample size between 7 and 17[35,37,67–71]. In addition, post-hoc power analysis (G-power 3.1) revealed that, for all significant ANOVA effects in our study, values of Power (1-β err prob) are >0.95. All of the participants had normal or corrected-to-normal vision and met TMS safety criteria by self-report. All participants gave written informed consent before taking part in the study, which was conducted in accordance with the Declaration of Helsinki and approved by the local ethics committee. Here, subjects were randomly assigned to one of three groups, with distinct stimulation protocols (see Methods details section): IAF-1Hz (group 1=mean age 22.64±0.52, nine females), IAF (group 2=mean age 23.88 ± 0.52, eight females) and IAF+1Hz (group 3=mean age 23.88±0.77, eight females), each containing 17 participants.

Experiment 3

Participants. Seventeen healthy new volunteers (12 women, 5 men; mean age=22.47, SE=0.66) were recruited for Experiment 3.

Method details

Experiment 1

Stimuli and task procedure. Participants were comfortably seated in front of a CRT monitor (100Hz refresh rate) at a viewing distance of 57cm. A PC running E-Prime software (Psychology Software Tools, Inc., USA) controlled stimulus presentation and responses registration. During the main experimental procedure (main task), each trial consisted of a *primary visual detection task*, in which participants responded to visual stimuli displayed on the computer screen, and a *secondary confidence task*, in which participants rated the level of confidence in their perception on a scale of 1 to 4, where 1=no confidence at all; 2=little confidence; 3=moderate confidence; and 4=high confidence. At the beginning of each trial, a white fixation cross was displayed on a grey background. The fixation cross was presented in the centre of the screen for 2000ms and subtended a visual angle of 0.8°. Afterwards, an X (visual angle 2°) was created by rotating the fixation cross by 45 degrees. The cue appeared for a variable time period (time jitter between 2000 and 3000ms), immediately followed by the primary task stimulus. The stimulus could appear with equal probability on the right or left visual field. These stimuli were presented at 4.1°/3.7° eccentricity (horizontal/vertical) in the lower part of the left visual field (LVF) or right visual field (RVF) for 60ms. The primary task stimulus could be either a catch stimulus (50% of trials) or a target stimulus (50% of trials). Catch stimuli consisted of 8x8 black and white checkerboards (height=4cm; width=4cm. visual angle=15.9°). Target stimuli consisted of the same checkerboard containing iso-luminant grey circles, which contrasted the black and white parts of the checkerboard. Participants were prompted to press the spacebar on the keyboard with their right index finger whenever they detected the circles embedded in the checkerboard. Primary response speed was not stressed over perceptual accuracy, but a time limit of 2000ms was given. After this primary response, confidence ratings were collected. The Italian version of the question: “How confident are you about your percept?” was presented until participants rated their confidence. Confidence was rated on a 4-points Likert scale, from “no confidence at all” to “high confidence”, and was reported by pressing the corresponding number on the keyboard with the left index finger. Notably, here the confidence rating reflects a participant’s level of subjective certainty in having correctly perceived the stimulus[72]. After rating their confidence, a new trial started with the presentation of a new fixation cross. The main task consisted of 5 blocks with 60 trials per block (total trial number=300) and lasted on average 90min.

Titration session. A titration session was run before the main experimental session in order to set stimuli contrast ratios corresponding to each individual’s 50% perceptual threshold. Iso-luminant circles of 8 different contrast ratios (RGB contrasts on black/white background: 28/227, 32/223, 36/219, 40/215, 44/211, 48/207 and 100/155) were presented together with catch trials (checkerboards without iso-luminant circles). Please note examples of stimuli of different contrasts: A. Catch Stimulus B. Low Contrast Stimulus (RGB contrasts: 30/225) C. High Contrast Stimulus (RGB contrasts:40/215) D. Maximum Contrast Stimulus (RGB contrasts:100/155).

To account for individual biases among participants in their response to catch trials, a false alarm rate was considered, together with target stimuli of different contrast for the calculation of the sigmoid function. For each iso-luminant contrast, individual performance was then entered to calculate the sigmoid function.

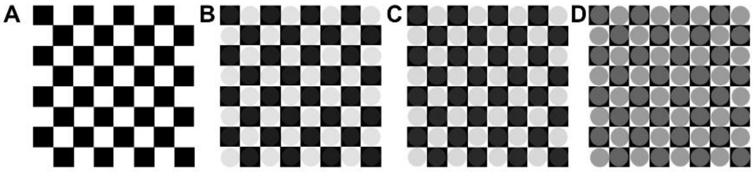

Figure 6. Examples of stimuli of different contrasts. A. Catch Stimulus **B.** Low Contrast Stimulus (RGB contrasts: 30/225) **C.** High Contrast Stimulus (RGB contrasts:40/215) **D.** Maximum Contrast Stimulus (RGB contrasts:100/155)

Data were analyzed using the following formula to calculate the threshold value (y):

$$y = \frac{100}{1 + \mathrm{e}^{-\frac{x-c}{d}}}$$

Where x is the contrast value, c is the inflection point of the curve and d is the slope of the sigmoid.

The corresponding inflection point was selected as the bias-adjusted threshold, which was used for stimulus presentation during the experiment. In Experiment 1, detection performance threshold during the main task (M=56.9%, SE=3.69%) was not statistically different form the bias-adjusted threshold (M=51.58%, SE=0.48%) calculated during the titration session, (*t*(24)=1.68, *p*=.11, *d*=0.34). Across participants, the selected luminance contrast ratios during the main task ranged between 20/235 and 50/205 RGB points (M=32/223, SE=12).

Experiment 2

Both Experiment 2 and Experiment 3 implemented a rhythmic-TMS entrainment protocol with concurrent EEG recording. The timing of rhythmic-TMS pulses differed between the two experiments.

Stimuli and task procedure. Stimuli and tasks in Experiment 2 were the same as those described for Experiment 1, with the main difference being the active manipulation of alpha activity via an entrainment protocol.

Entrainment of the intrinsic oscillatory alpha activity was achieved using rhythmic transcranial magnetic stimulation (rhythmic-TMS). Specifically, pre-stimulus alpha activity was fine-tuned relative to individual alpha-frequency using rhythmic five-pulse TMS bursts in which the time lag between pulses was manipulated depending on the group[21,73]. In order to induce changes in the alpha-frequency cycle length, rhythmic-TMS was applied at a slower or faster pace, relative to a participant's individual alpha-frequency. To selectively modulate alpha-amplitude, the frequency of the rhythmic-TMS pulse trains was matched to the intrinsic individual alpha-frequency of the participant, thus enhancing the synchronization of neural firing and phase alignment without influencing the speed of alpha activity. In this way, rhythmic-TMS pulse trains could occur at three different frequencies: at the individual alpha-frequency of the participant to manipulate pre-stimulus alpha-amplitude (IAF group); at 1Hz lower than the individual alpha-frequency (IAF-1Hz group) to slow-down pre-stimulus alpha-frequency; or at 1Hz higher than the individual alpha-frequency (IAF+1Hz group) to speed-up pre-stimulus alpha-frequency. In all groups, the last TMS-pulse coincided with the stimulus appearance.

Biphasic stimulation was applied using a Magstim Rapid Transcranial Magnetic Stimulator via a 70mm figure-of-eight coil (Magstim Company, UK) of maximum field strength ~1.55T. As systematic differences in visual cortex excitability do not seem to be present between the hemispheres[34,74–76], TMS bursts were delivered only to the right occipital site (at O2 electrode position), with the coil surface tangent to the scalp, and the handle oriented perpendicular to the medial plane of the subjects head (latero-medial current direction). Moreover, pulse intensity was kept fixed at 60% of the maximum stimulator output (MSO)[34,77–79], roughly corresponding to previously reported phosphene thresholds[80–84]. No subject reported to have perceived phosphenes during the execution of the task. Within-subject sham control stimulation was implemented in order to account for any non-specific rhythmic-TMS effects. To do so, a modified coil was used that provided enough distance from the scalp to ensure the absence of stimulation, while at the same time maintaining coil position, as well as tactile and acoustic sensations. Each participant underwent three consecutives rhythmic-TMS and sham blocks (resulting in a total of 900 active rhythmic-TMS pulses), whereas rhythmic-TMS/sham stimulation block order was randomized. Therefore, the experimental session consisted of 6 blocks with 60 trials per block (total trial number=360) (see also Experiment 1), with short breaks between the blocks (overall average task duration of 50 minutes). The rhythmic-TMS design was in line with current safety guidelines[85].

Titration session. Titration was run as for Experiment 1. Additionally, in the second experiment, during the titration session, individual alpha peak frequency (defined as the maximum local power in the alpha-frequency range) was determined. A total of six minutes resting-state EEG (three minutes with eye closed and three minutes with eyes open, and with gaze on a fixation cross on the screen) was recorded from 8 Ag/AgCl parieto-occipital electrodes (O1,P3,PO3,PO7; O2,P4,PO4, PO8). Individual alpha-frequency peak was calculated from the power spectra of the eyes open condition, applying a Fast Fourier Transformation. In line with Experiment 1 (showing a local alpha power maxima over O2) and previous studies, alpha-frequency was calculated from the O2 electrode[21,83], over which rhythmic-TMS was subsequently applied (see above). The identified individual alpha-frequency was used to calibrate rhythmic-TMS frequency.

Experiment 3

Stimuli and task procedure. The stimuli and task for Experiment 3 were the same as those used for Experiment 2, the main difference being the timing of the manipulation of alpha activity via an entrainment protocol.

Specifically, Experiment 3 aimed to selectively enhance post-stimulus alpha-amplitude, prior to the confidence prompt. As such, only one entrainment protocol was applied (i.e. stimulation at the individual alpha-frequency). While in Experiment 2, the final pulse of the rhythmic-TMS-train coincided with stimulus onset, in Experiment 3, the final rhythmic-TMS pulse coincided with the onset of the confidence prompt.

Stimulation site, coil orientation, stimulation intensity, control conditions and number of pulses were the same as those used in Experiment 2.

Titration session. The titration session was conducted as in Experiment 2.

Quantification and Statistical Analysis

Experiment 1

Psychophysiological recording – paradigm and acquisition. EEG data were collected during the main task in Experiment 1 from 64 Ag/AgCl electrodes

(Fp1,Fp2,AF3,AF4,AF7,AF8,F1,F2,F3,F4,F7,F8,FC1,FC2,FC3,FC4,FC5,FC6,FT7,FT8,C1,C2,C3,C4,C5,C6,T7,T8,CP1,CP2,CP3,CP4,CP5,CP6,TP7,TP8,P1,P2,P3,P4,P5,P6,P7,P8,PO3,PO4,PO7,PO8,O1,O2,Fpz,AFz,Fz,FCz,Cz,CPz,Pz,POz,Oz) and from the right mastoid with Brain Vision recorder software (Brain Products, Munich, Germany). The left mastoid was used as reference, and the ground electrode was placed on the right cheek. The electrooculogram (EOG) was recorded from above and below the left eye and from the outer canthi of both eyes. EEG and EOG were recorded with a band-pass filter of 0.01–100Hz, at a sampling rate of 1000Hz, which was re-sampled to 500Hz offline. The impedance of all electrodes was kept below 10kΩ. EEG data were pre-analyzed using custom made routines in MatLab R2013b (The Mathworks, Natick, MA, USA). EEG data were re-referenced off-line to the average of all electrodes and filtered with a 0.5–30Hz pass-band. Epochs were extracted stimulus-locked from -1500ms to 2500ms. Artefact-contaminated epochs were excluded using the pop_autorej function in EEGLAB v13.0.1[86], which first excludes trials with voltage fluctuations larger than 1000 µV, and then excludes trials with data values outside five standard deviations (mean=9.7% SE=2.9% of trials removed). Subsequently, EOG artefacts were corrected by a procedure based on a linear regression method (lms_regression function in MatLab R2013b)[87]. Because perceptually relevant, pre-stimulus alpha activity shows hemispheric lateralization, relative to upcoming stimulus location, we recoded electrode positions as contralateral versus ipsilateral to the hemifield of stimulus presentation (resulting in all contralateral activity being on one side, which was conventionally defined to be the right), i.e. for RVF-stimulus epochs, data from the contralateral (left) electrodes were copied and flipped to right-sided electrodes, electrodes on the midline were not flipped or recoded.

In order to identify the individual alpha-frequency peak during the task, data epochs in the cue-stimulus period (i.e. pre-stimulus alpha from -1000ms to stimulus presentations, baseline between -1500 and -1000ms) were analyzed with a fast Fourier transformation (MatLab function spectopo, frequency resolution: 0.166Hz). Power was calculated separately for each subject and condition and was normalized by z-score decibel (dB=10*log10[-power/baseline]) transformation at each frequency. Individual alpha-frequency was defined as the local maximum power within the frequency range 7-13Hz (i.e. alpha peak). Each subject showed a clear peak within this alpha range. However, a peak in the alpha-band was not present at all electrodes. For this reason, power spectra on all parietal-occipital electrodes were visually inspected. Then, the contralateral electrode was selected for analyses where alpha oscillation showed a clear peak[23]. Homologous electrodes were selected for the analyses in the ipsilateral hemisphere. This procedure identified the following subset of parieto-occipital electrodes that were used separately for each subject and condition to identify alpha-frequency in the cue-stimulus period: contralateral electrodes (P8,PO8,PO4,O2), and ipsilateral electrodes (P7,PO7,PO3,O1). Importantly, most of the participants (n=15) showed maximum power over electrode O2.

The amplitude of alpha oscillations was calculated by time-frequency analyses of data epoched from 2000ms before to 2000ms after the stimulus onset. Long epochs prevent edge artefacts from contaminating time frequency power in the time windows of interest. Spectral EEG activity was assessed by time-frequency decomposition using a complex sinusoidal wavelet convolution procedure (between 2 and 25 cycles per wavelet, linearly increasing across 50 linear-spaced frequencies from 2.0Hz to 50.0Hz) with the newtimef function from EEGLAB v13.0.1[86] and custom routines in MatLab. The resulting power was normalized by decibel (dB=10*log10[-power/baseline]) transformation at each frequency, using a single trial baseline between -1000 and -500 preceding stimulus onset. This long baseline window was used to increase the signal-to-noise ratio during the baseline period and is frequently applied in time frequency analyses[88,89]. This procedure was applied separately for each subject and condition. Mean alpha (7-13Hz) amplitude was computed separately for each condition in the cue-stimulus interval (-500 to 0ms)[18] and in the post-stimulus interval (0 to 900ms), which corresponds to the pre-confidence prompt time period. In order to identify electrode clusters for the analyses of alpha-amplitude, we used the same procedure as for alpha-frequency. For alpha-amplitude, the following subsets of posterior contralateral (P2,P4,P8,PO4,PO8,O2) and ipsilateral (P1,P3,P7,PO3,PO7,O1) electrodes were used for the analyses. Importantly, as for alpha-frequency, most of the participants (n=18) showed maximum alpha-amplitude over electrode O2.

Statistical Analyses. First, trials were sorted according to objective accuracy (i.e. into correct and error trials). Correct trials consisted of correctly detected target trials (i.e. hits, where participants pressed the spacebar after a target trial) and correctly detected catch trials (i.e. correct rejections, where participants did not press the spacebar after a catch trial). Accordingly, error trials consisted of misses after target trials and false alarms after catch trials. Then we compared participants with high vs low perceptual sensitivity. Perceptual sensitivity was estimated using the *d'* measure. In signal detection theory (SDT[28]), *d'* reflects standardized measure of discrimination abilities between the signal and the noise (type I sensitivity). *d'* was calculated as $d'=z(\mathrm{H}) - z(\mathrm{FA})$, where z represents the z-scores of Hit rate (i.e. H, the probability of correct reactions on target trials) and false alarms (i.e. FA, the probability of incorrect reactions on catch trials[28]).

Next, we focused on subjective confidence levels during correct trials (i.e. hits and correct rejections). In order to compare confident vs. non-confident responses, we aggregated high confident responses and low confident responses. In this way, correct trials were dived in high confident (i.e. with a confidence rating of 3 or 4) and low confident (i.e. with a confidence rating of 1 or 2) trials. Then, we compared participants showing high vs low confidence or metacognitive performance. For confidence analyses, the mean value of the confidence ratings was calculated for each participant. Instead, metacognitive performance was quantified using the computational method proposed by Maniscalco & Lau[29]. This method quantifies the efficacy of confidence ratings to discriminate between correct and erroneous responses in a SDT model. The model accounts for the variance in task performance to compute metacognitive sensitivity (type II sensitivity) on subjective confidence rating. This method, previously described in detail and validated, can give a metric (termed *meta-d*') for metacognitive abilities[29,90]. Briefly, the central idea is to link type I and type II SDT models to compute the observed type II sensitivity. *meta-d'* estimates the values, which maximize the fit between the observed type II data and the parameter values of the *d*' type I SDT model. Here, *meta-d*' was calculated with the function fit_meta_d_SSE in MatLab. This function minimizes the sum of squared errors and estimates *meta-d'* using observed type II data and the empirical type I criterion *c'* [90]. In this way, *meta-d*' estimates, for instance, the relative likelihood to report a high confidence rating after a correct response[29,90]. Higher values of *meta-d*' correspond to participants having better metacognitive abilities.

Within participants EEG analyses were performed separately for objective accuracy and subjective confidence. For *Objective Accuracy*, we compared alpha activity (both frequency and amplitude) in 2x2 repeated measures ANOVAs with the factors ACCURACY (correct and incorrect) and HEMISPHERE (contralateral and ipsilateral). For Subjective Confidence, analyses were performed on correct trials[65]. Alpha activity was analyzed for the factor CONFIDENCE (high and low confidence) and for the factor HEMISPHERES (contralateral and ipsilateral) in 2x2 repeated measures ANOVAs. Differences between conditions were tested by one or two-tailed t-tests (planned comparisons).

Between participants EEG analyses were performed on perceptual sensitivity and metacognitive performance. For perceptual sensitivity analyses, we divided participants in two numerically equivalent groups using the median split of the d' scores (high vs low d'). As for perceptual sensitivity, we also conducted between-group analysis, by dividing participants in two numerically equivalent groups (high vs low meta d' scores) on a median split basis of the meta-d' scores (i.e. metacognitive performance). Differences between groups were tested by one or two-tailed independent samples t-tests (planned comparisons).

Pre-stimulus IAF and resting-state IAF. As we have used resting IAF to target pre-stimulus activity in experiments 2 and 3 (see results sections), we checked for any potential difference between resting-state IAF and pre-stimulus IAF in Experiment 1 to ensure adequacy of our approach, with the working hypothesis that no significant differences should be observed. In this analysis, resting-state IAF was defined as the maximum local power in the alpha-frequency range during the resting state over a cluster of posterior electrodes (O1,P1,P3,P5,P7,Pz,POz,Oz,PO3,PO7;

O2,P2,P4,P6,P8,PO4,PO8), while pre-stimulus IAF was calculated in the same electrode cluster across conditions in a time window between -1000ms and stimulus presentation. The analysis was performed on 22 out of 24 participants as resting EEG was not available for 2 participants. As expected, the two-tailed paired samples t-test showed no differences (t(21)=0.05, p=.968, d=.019) between resting state IAF (M=10.81Hz; SE=0.21Hz) and pre-stimulus IAF (M=10.83Hz; SE=0.37Hz). Importantly, these results demonstrate that resting-state IAF and pre-stimulus IAF are comparable within group.

Experiment 2

EEG recordings –acquisition and processing. EEG data were collected for Experiment 2 as for Experiment 1. However, in Experiment 2, a rhythmic-TMS pulse train was applied during EEG recording. The resulting rhythmic-TMS artefacts were identified and removed using an open-source EEGLab extension, the TMS-EEG signal analyzer (TESA)[91]. First, EEG data were epoched around stimulus onset (between -1500ms and 2500ms for Experiment 2 and between -1000ms and 2000ms for Experiment 3, due to differences in stimulation timing) and the linear trend from the obtained epochs was removed. Then rhythmic-TMS pulse artefact and peaks of rhythmic-TMS-evoked scalp muscle activities were removed (-10ms +10ms) and cubic interpolation was performed prior to down-sampling the data (from 5000Hz to 1000Hz). Interpolated data was again removed prior to Individual Component Analysis (ICA). Specifically, a fastICA algorithm was used (pop_tesa_fastica function: http://research.ics.aalto.fi/ica/fastica/code/dlcode.shtml) to identify individual components representing artefacts, along with automatic component classification (pop_tesa_compselect function), where each component was subsequently manually checked and reclassified when necessary. In this first round of ICA, only components with large amplitude artefacts, such as rhythmic-TMS-evoked scalp muscle artefacts, were eliminated. Data were again interpolated prior to applying pass-band (between 1 and 100Hz) and stop-band (between 48 and 52Hz) Butterworth filters. Subsequently interpolated data were again removed prior to the second round of ICA, in order to remove all other artefacts, such as blinks, eye movement, persistent muscle activity and electrode noise. Then, rhythmic-TMS-pulse period was interpolated and data was re-referenced to the average of all electrodes. Finally, single trials were visually inspected and those containing residual rhythmic-TMS artefact were removed. The described rhythmic-TMS artefact removal procedure was applied to all EEG data, both for active rhythmic-TMS and sham stimulations. On average, approximately one third of all epochs were removed (M=34.31%, SE=1.72%) (remaining epochs mean=236.5 epochs, SE=6.19). A graphical explanation of the artefact correction procedure is reported in the supplemental information (see supplemental figure S3).

Alpha-frequency and alpha-amplitude were identified in a similar manner as per Experiment 1. Alpha-frequency was defined as the local maximum power within the frequency 7-13Hz range in a pre-stimulus period (-650ms to stimulus presentation). Accordingly, pre-stimulus alpha-amplitude was calculated in the time frequency data (as for Experiment 1). The time window of analyses corresponded to stimulation period for both alpha-frequency and -amplitude. Near-stimulation parieto-occipital electrodes in the right hemisphere (PO4,PO8,O2), along with analogous electrodes in the left hemisphere (PO3,PO7,O1) were used for all of the analyses.

Statistical analyses (behavioral data). Behavioral data were analyzed separately for perceptual sensitivity (d' score) and for confidence (mean of confidence ratings) and metacognitive performance (meta d' score).

All scores were compared between the two HEMIFIELDs (left and right) and two STIMULATION types (active rhythmic-TMS and sham) in three GROUPs of participants (IAF±1Hz, IAF), in 2x2x3 repeated measures mixed-model ANOVAs.

Statistical analyses (EEG data). Electrophysiological data were analyzed separately for pre-stimulus alpha-amplitude and alpha-frequency. Therefore, both parameters of alpha activity were compared between the two HEMISPHERES (left and right parieto-occipital cluster) and the two STIMULATION types (active rhythmic-TMS and sham) in three GROUPs of participants in 2x2x3 repeated measures mixed-model ANOVAs. Differences between conditions were tested by two-tailed t-test (planned comparisons).

Finally, the association between rhythmic-TMS-evoked differences in alpha-frequency in the stimulated (right) hemisphere (computed as a difference in alpha-frequency between active rhythmic-TMS and sham stimulation conditions) and differences in perceptual sensitivity in the opposite (left) hemispace (computed as a difference in d' score between active rhythmic-TMS and sham stimulation conditions) was explored via linear regression.

Experiment 3

EEG recordings – acquisition and processing. EEG data were recorded and alpha-frequency and alpha-amplitude identified as in Experiments 1 and 2, with the only difference being that the analysis window was moved to a time window preceding the confidence prompt (850ms to 1500ms after stimulus presentation, which corresponded to -650ms prior to the confidence prompt).

Statistical analyses (behavioral data). Behavioral data were analyzed separately for perceptual sensitivity (d’ score) and for confidence (mean of confidence ratings) and metacognitive performance (meta d’ score). All scores were compared for the two HEMIFIELDS (left and right) and between different STIMULATION types (active rhythmic-TMS and sham) in a 2x2 repeated measures ANOVA.

Statistical analyses (EEG data). Electrophysiological data were analyzed separately for alpha-amplitude and alpha-frequency. Moreover, differences in alpha-amplitude and alpha-frequency were again compared between the two HEMISPHERES (left and right) and between STIMULATION types (active rhythmic-TMS and sham) in a 2x2 repeated measures ANOVA. Differences between conditions were tested by two-tailed t-test (planned comparisons).

Finally, a linear regression model was used to determine whether rhythmic-TMS-evoked differences in alpha-amplitude in the stimulated (right) hemisphere (computed as a difference in alpha-amplitude between active rhythmic-TMS and sham stimulation conditions) can predict differences in confidence levels in the opposite (left) hemifield (computed as a difference in meta d’ scores between active rhythmic-TMS and sham stimulation conditions).

References

1. Hirst, W., Phelps, E.A., Meksin, R., Vaidya, C.J., Johnson, M.K., Mitchell, K.J., Buckner, R.L., Budson, A.E., Gabrieli, J.D.E., Lustig, C., et al. (2015). A ten-year follow-up of a study of memory for the attack of September 11, 2001: Flashbulb memories and memories for flashbulb events. Journal of Experimental Psychology: General *144*, 604–623.
2. Garry, M., Manning, C.G., Loftus, E.F., and Sherman, S.J. (1996). Imagination inflation: Imagining a childhood event inflates confidence that it occurred. Psychonomic Bulletin and Review *3*, 208–214.
3. Ferri, F., Venskus, A., Fotia, F., Cooke, J., and Romei, V. (2018). Higher proneness to multisensory illusions is driven by reduced temporal sensitivity in people with high schizotypal traits. Consciousness and Cognition *65*, 263–270.
4. Fenner, B., Cooper, N., Romei, V., and Hughes, G. (2020). Individual differences in sensory integration predict differences in time perception and individual levels of schizotypy. Consciousness and Cognition *84*, 102979.
5. Köther, U., Lincoln, T.M., and Moritz, S. (2018). Emotion perception and overconfidence in errors under stress in psychosis. Psychiatry Research *270*, 981–991.
6. Klimesch, W., Sauseng, P., and Hanslmayr, S. (2007). EEG alpha oscillations: The inhibition-timing hypothesis. Brain Research Reviews *53*, 63–88.
7. Mazaheri, A., and Jensen, O. (2010). Rhythmic pulsing: linking ongoing brain activity with evoked responses. Frontiers in Human Neuroscience *4*, 1–13.
8. Palva, S., and Palva, J.M. (2007). New vistas for α-frequency band oscillations. Trends in Neurosciences *30*, 150–158.
9. Samaha, J., Iemi, L., Haegens, S., and Busch, N.A. (2020). Spontaneous Brain Oscillations and Perceptual Decision-Making. Trends in Cognitive Sciences *24*, 639–653.
10. Zazio, A., Schreiber, M., Miniussi, C., and Bortoletto, M. (2020). Modelling the effects of ongoing alpha activity on visual perception: The oscillation-based probability of response. Neuroscience and Biobehavioral Reviews *112*, 242–253.
11. Zoefel, B., and VanRullen, R. (2017). Oscillatory mechanisms of stimulus processing and selection in the visual and auditory systems: State-of-the-art, speculations and suggestions. Frontiers in Neuroscience *11*, 1–13.
12. VanRullen, R. (2016). Perceptual Cycles. Trends in Cognitive Sciences *20*, 723–735.
13. Wutz, A., and Melcher, D. (2014). The temporal window of individuation limits visual capacity. Frontiers in Psychology *5*, 1–14.
14. Jensen, O., Gips, B., Bergmann, T.O., and Bonnefond, M. (2014). Temporal coding organized by coupled alpha and gamma oscillations prioritize visual processing. Trends in Neurosciences *37*, 357–369.
15. Busch, N.A., and VanRullen, R. (2010). Spontaneous EEG oscillations reveal periodic sampling of visual attention. Proceedings of the National Academy of Sciences *107*, 16048–16053.
16. Romei, V., Brodbeck, V., Michel, C., Amedi, A., Pascual-Leone, A., and Thut, G. (2008). Spontaneous fluctuations in posterior α-band EEG activity reflect variability in excitability of human visual areas. Cerebral Cortex *18*, 2010–2018.
17. Benwell, C.S.Y., Tagliabue, C.F., Veniero, D., Cecere, R., Savazzi, S., and Thut, G. (2017). Pre-stimulus EEG power predicts conscious awareness but not objective visual performance. Eneuro *4*, ENEURO.0182-17.2017.
18. Samaha, J., Iemi, L., and Postle, B.R. (2017). Prestimulus alpha-band power biases visual discrimination confidence, but not accuracy. Consciousness and Cognition *54*, 47–55.
19. Iemi, X.L., Chaumon, M., Se, X., Crouzet, M., and Busch, X.N.A. (2017). Spontaneous Neural Oscillations Bias Perception by Modulating Baseline Excitability.

Journal of Neuroscience *37*, 807–819.

20. Limbach, K., and Corballis, P.M. (2016). Prestimulus alpha power influences response criterion in a detection task. Psychophysiology *53*, 1154–1164.

21. Cecere, R., Rees, G., and Romei, V. (2015). Individual differences in alpha frequency drive crossmodal illusory perception. Current Biology *25*, 231–235.

22. Minami, S., and Amano, K. (2017). Illusory Jitter Perceived at the Frequency of Alpha Oscillations. Current Biology *27*, 2344–2351.

23. Samaha, J., and Postle, B.R. (2015). The Speed of Alpha-Band Oscillations Predicts the Temporal Resolution of Visual Perception. Current Biology *25*, 2985–2990.

24. Wutz, A., Melcher, D., and Samaha, J. (2018). Frequency modulation of neural oscillations according to visual task demands. Proceedings of the National Academy of Sciences of the United States of America *115*, 1346–1351.

25. Cooke, J., Poch, C., Gillmeister, H., Costantini, M., and Romei, V. (2019). Oscillatory Properties of Functional Connections Between Sensory Areas Mediate Cross-Modal Illusory Perception. The Journal of neuroscience : the official journal of the Society for Neuroscience *39*, 5711–5718.

26. Migliorati, D., Zappasodi, F., Perrucci, M.G., Donno, B., Northoff, G., Romei, V., and Costantini, M. (2020). Individual Alpha Frequency Predicts Perceived Visuotactile Simultaneity. Journal of Cognitive Neuroscience *32*, 1–11.

27. Mierau, A., Klimesch, W., and Lefebvre, J. (2017). State-dependent alpha peak frequency shifts: Experimental evidence, potential mechanisms and functional implications. Neuroscience.

28. Green, D.M., and Swets, J.A. (1966). Signal detection theory and psychophysics. John Wiley, ed. (Oxford, England).

29. Maniscalco, B., and Lau, H. (2012). A signal detection theoretic approach for estimating metacognitive sensitivity from confidence ratings. Consciousness and Cognition.

30. Yeung, N., and Summerfield, C. (2012). Metacognition in human decision-making: confidence and error monitoring. Philosophical Transactions of the Royal Society B: Biological Sciences *367*, 1310–1321.

31. Murphy, P.R., Robertson, I.H., Harty, S., and O'Connell, R.G. (2015). Neural evidence accumulation persists after choice to inform metacognitive judgments. eLife, 1–23.

32. Pleskac, T.J., and Busemeyer, J.R. (2010). Two-stage dynamic signal detection: A theory of choice, decision time, and confidence. Psychological Review *117*, 864–901.

33. Iemi, L., Busch, N.A., Laudini, A., Haegens, S., Samaha, J., Villringer, A., and Nikulin, V. V. (2019). Multiple mechanisms link prestimulus neural oscillations to sensory responses. eLife *8*, 1–34.

34. Romei, V., Thut, G., Mok, R.M., Schyns, P.G., and Driver, J. (2012). Causal implication by rhythmic transcranial magnetic stimulation of alpha frequency in feature-based local vs. global attention. The European journal of neuroscience *35*, 968–974.

35. Romei, V., Driver, J., Schyns, P.G., and Thut, G. (2011). Rhythmic TMS over Parietal Cortex Links Distinct Brain Frequencies to Global versus Local Visual Processing. Current Biology *21*, 334–337.

36. Romei, V., Thut, G., and Silvanto, J. (2016). Information-Based Approaches of Noninvasive Transcranial Brain Stimulation. Trends in Neurosciences *39*, 782–795.

37. Thut, G., Veniero, D., Romei, V., Miniussi, C., Schyns, P., and Gross, J. (2011). Rhythmic TMS causes local entrainment of natural oscillatory signatures. Current Biology *21*, 1176–1185.

38. Helfrich, R.F., Schneider, T.R., Rach, S., Trautmann-Lengsfeld, S.A., Engel, A.K., and Herrmann, C.S. (2014). Entrainment of brain oscillations by transcranial alternating current stimulation. Current Biology *24*, 333–339.

39. Thut, G., Bergmann, T.O., Fröhlich, F., Soekadar, S.R., Brittain, J.S., Valero-Cabré, A., Sack, A.T., Miniussi, C., Antal, A., Siebner, H.R., et al. (2017). Guiding transcranial brain stimulation by EEG/MEG to interact with ongoing brain activity and associated functions: A position paper. Clinical Neurophysiology *128*, 843–857.

40. Veniero, D., Vossen, A., Gross, J., and Thut, G. (2015). Lasting EEG/MEG aftereffects of rhythmic transcranial brain stimulation: Level of control over oscillatory network activity. Frontiers in Cellular Neuroscience *9*, 1–17.

41. Romei, V., Bauer, M., Brooks, J.L., Economides, M., Penny, W., Thut, G., Driver, J., and Bestmann, S. (2016). Causal evidence that intrinsic beta-frequency is relevant for enhanced signal propagation in the motor system as shown through rhythmic TMS. NeuroImage *126*, 120–130.

42. Ergenoglu, T., Demiralp, T., Bayraktaroglu, Z., Ergen, M., Beydagi, H., and Uresin, Y. (2004). Alpha rhythm of the EEG modulates visual detection performance in humans. Cognitive Brain Research *20*, 376–383.

43. van Dijk, H., Schoffelen, J.-M., Oostenveld, R., and Jensen, O. (2008). Prestimulus Oscillatory Activity in the Alpha Band Predicts Visual Discrimination Ability. Journal of Neuroscience *28*, 1816–1823.

44. Roberts, D.M., Fedota, J.R., Buzzell, G.A., Parasuraman, R., and McDonald, C.G. (2014). Prestimulus Oscillations in the Alpha Band of the EEG Are Modulated by the Difficulty of Feature Discrimination and Predict Activation of a Sensory Discrimination Process. Journal of Cognitive Neuroscience *26*, 1615–1628.

45. Baumgarten, T.J., Schnitzler, A., and Lange, J. (2016). Prestimulus Alpha Power Influences Tactile Temporal Perceptual Discrimination and Confidence in Decisions. Cerebral Cortex *26*, 891–903.

46. Iemi, L., and Busch, N.A. (2018). Moment-to-Moment Fluctuations in Neuronal Excitability Bias Subjective Perception Rather than Strategic Decision-Making. Eneuro *5*, 1–13.

47. Weisz, N., Lüchinger, C., Thut, G., and Müller, N. (2014). Effects of individual alpha rTMS applied to the auditory cortex and its implications for the treatment of chronic tinnitus. Hum Brain Mapp *35*, 14–29.

48. Hanslmayr, S., Matuschek, J., and Fellner, M.-C. (2014). Entrainment of prefrontal beta oscillations induces an endogenous echo and impairs memory formation. Curr Biol *24*, 904–909.

49. Varela, F.J., Toro, A., Roy John, E., and Schwartz, E.L. (1981). Perceptual framing and cortical alpha rhythm. Neuropsychologia *19*, 675–686.

50. Mathewson, K.E., Gratton, G., Fabiani, M., Beck, D.M., and Ro, T. (2009). To See or Not to See: Prestimulus Phase Predicts Visual Awareness. Journal of Neuroscience *29*, 2725–2732.

51. Dugué, L., Marque, P., and VanRullen, R. (2011). The phase of ongoing oscillations mediates the causal relation between brain excitation and visual perception. Journal of Neuroscience *31*, 11889–11893.

52. Busch, N.A., Dubois, J., and VanRullen, R. (2009). The phase of ongoing EEG oscillations predicts visual perception. Journal of Neuroscience *29*, 7869–7876.

53. Haegens, S., Nácher, V., Luna, R., Romo, R., and Jensen, O. (2011). α-Oscillations in the monkey sensorimotor network influence discrimination performance by rhythmical inhibition of neuronal spiking. PNAS *108*, 19377–19382.

54. Navajas, J., Bahrami, B., and Latham, P.E. (2016). Post-decisional accounts of biases in confidence. Current Opinion in Behavioral Sciences *11*, 55–60.

55. Fleming, S.M., and Daw, N.D. (2017). Self-Evaluation of Decision-Making: A General Bayesian Framework for Metacognitive Computation. Psychol Rev *124*, 91–114.

56. Pereira, M., Faivre, N., Iturrate, I., Wirthlin, M., Serafini, L., Martin, S., Desvachez, A., Blanke, O., Van De Ville, D., and Millán, J. del R. (2020). Disentangling the origins of confidence in speeded perceptual judgments through multimodal imaging. Proc Natl Acad Sci USA *117*, 8382–8390.

57. Posner, M.I., Snyder, C.R., and Davidson, B.J. (1980). Attention and the detection of signals. Journal of Experimental Psychology: General *109*, 160–174.

58. Fan, J., McCandliss, B.D., Sommer, T., Raz, A., and Posner, M.I. (2002). Testing the Efficiency and Independence of Attentional Networks. Journal of Cognitive Neuroscience *14*, 340–347.

59. Thut, G., Nietzel, A., Brandt, S., and Pascual-Leone, A. (2006). Alpha Band Electroencephalographic Activity over Occipital Cortex Indexes Visuospatial Attention Bias and Predicts Visual Target Detection. Journal of Neuroscience *13*, 9494–9502.

60. Rihs, T.A., Michel, C.M., and Thut, G. (2007). Mechanisms of selective inhibition in visual spatial attention are indexed by α-band EEG synchronization. European Journal of Neuroscience *25*, 603–610.

61. Tarasi, L., Trajkovic, J., Diciotti, S., di Pellegrino, G., Ferri, F., Ursino, M., and Romei, V. (2021). Predictive waves in the autism-schizophrenia continuum: A novel biobehavioral model. Neurosci Biobehav Rev *132*, 1–22.

62. Haegens, S., Cousijn, H., Wallis, G., Harrison, P.J., and Nobre, A.C. (2014). Inter- and intra-individual variability in alpha peak frequency. NeuroImage.

63. Hülsdünker, T., Mierau, A., and Strüder, H.K. (2016). Higher balance task demands are associated with an increase in individual alpha peak frequency. Frontiers in Human Neuroscience.

64. Maurer, U., Brem, S., Liechti, M., Maurizio, S., Michels, L., and Brandeis, D. (2014). Frontal Midline Theta Reflects Individual Task Performance in a Working Memory Task. Brain Topography.

65. Samaha, J., Bauer, P., Cimaroli, S., and Postle, B.R. (2015). Top-down control of the phase of alpha-band oscillations as a mechanism for temporal prediction. Proceedings of the National Academy of Sciences of the United States of America *112*, 8439–8444.

66. Benwell, C.S.Y., Coldea, A., Harvey, M., and Thut, G. (2021). Low pre-stimulus EEG alpha power amplifies visual awareness but not visual sensitivity. European Journal of Neuroscience, 1–16.

67. Romei, V., Gross, J., and Thut, G. (2010). On the role of prestimulus alpha rhythms over occipito-parietal areas in visual input regulation: Correlation or causation? Journal of Neuroscience *30*, 8692–8697.

68. Albouy, P., Weiss, A., Baillet, S., and Zatorre, R.J. (2017). Selective Entrainment of Theta Oscillations in the Dorsal Stream Causally Enhances Auditory Working Memory Performance. Neuron *94*, 193-206.e5.

69. Vernet, M., Stengel, C., Quentin, R., Amengual, J.L., and Valero-Cabré, A. (2019). Entrainment of local synchrony reveals a causal role for high-beta right frontal oscillations in human visual consciousness. Scientific Reports *9*, 1–15.

70. Sauseng, P., Klimesch, W., Heise, K.F., Gruber, W.R., Holz, E., Karim, A.A., Glennon, M., Gerloff, C., Birbaumer, N., and Hummel, F.C. (2009). Brain Oscillatory Substrates of Visual Short-Term Memory Capacity. Current Biology *19*, 1846–1852.

71. Chanes, L., Quentin, R., Tallon-Baudry, C., and Valero-Cabré, A. (2013). Causal frequency-specific contributions of frontal spatiotemporal patterns induced by non-invasive neurostimulation to human visual performance. Journal of Neuroscience *33*, 5000–5005.

72. De Martino, B., Fleming, S.M., Garrett, N., and Dolan, R.J. (2013). Confidence in value-based choice. Nature neuroscience *16*, 105–10.

73. Wolinski, N., Cooper, N.R., Sauseng, P., and Romei, V. (2018). The speed of parietal

theta frequency drives visuospatial working memory capacity. PLoS Biology.

74. Bestmann, S., Ruff, C.C., Blakemore, C., Driver, J., and Thilo, K. V (2007). Spatial Attention Changes Excitability of Human Visual Cortex to Direct Stimulation. Current Biology *17*, 134–139.

75. Cattaneo, Z., Silvanto, J., Battelli, L., and Pascual-Leone, A. (2009). The mental number line modulates visual cortical excitability. Neurosci Lett *462*, 253–256.

76. Silvanto, J., and Muggleton, N.G. (2008). A novel approach for enhancing the functional specificity of TMS: Revealing the properties of distinct neural populations within the stimulated region. Clinical Neurophysiology *119*, 124.

77. Mevorach, C., Humphreys, G.W., and Shalev, L. (2006). Opposite biases in salience-based selection for the left and right posterior parietal cortex. Nature Neuroscience.

78. Pitcher, D., Walsh, V., Yovel, G., and Duchaine, B. (2007). TMS Evidence for the Involvement of the Right Occipital Face Area in Early Face Processing. Current Biology *17*, 1568–1573.

79. Silvanto, J., Lavie, N., and Walsh, V. (2005). Double dissociation of V1 and V5/MT activity in visual awareness. Cerebral Cortex *15*, 1736–1741.

80. Bolognini, N., Senna, I., Maravita, A., Pascual-Leone, A., and Merabet, L.B. (2010). Auditory enhancement of visual phosphene perception: The effect of temporal and spatial factors and of stimulus intensity. Neuroscience Letters.

81. Gerwig, M., Kastrup, O., Meyer, B.U., and Niehaus, L. (2003). Evaluation of cortical excitability by motor and phosphene thresholds in transcranial magnetic stimulation. Journal of the Neurological Sciences.

82. Romei, V., Murray, M.M., Cappe, C., and Thut, G. (2009). Preperceptual and Stimulus-Selective Enhancement of Low-Level Human Visual Cortex Excitability by Sounds. Current Biology *19*, 1799–1805.

83. Romei, V., Murray, M.M., Merabet, L.B., and Thut, G. (2007). Occipital transcranial magnetic stimulation has opposing effects on visual and auditory stimulus detection: Implications for multisensory interactions. Journal of Neuroscience *27*, 11465–11472.

84. Romei, V., Rihs, T., Brodbeck, V., and Thut, G. (2008). Resting electroencephalogram alpha-power over posterior sites indexes baseline visual cortex excitability. NeuroReport *19*, 203–208.

85. Rossi, S., Hallett, M., Rossini, P.M., and Pascual-Leone, A. (2009). Safety, ethical considerations, and application guidelines for the use of transcranial magnetic stimulation in clinical practice and research. Clin Neurophysiol *120*, 2008–2039.

86. Delorme, A., and Makeig, S. (2004). EEGLAB: An open source toolbox for analysis of single-trial EEG dynamics including independent component analysis. Journal of Neuroscience Methods.

87. Gratton, G., Coles, M.G.H., and Donchin, E. (1983). A new method for off-line removal of ocular artifact. Electroencephalography and Clinical Neurophysiology *55*, 468–484.

88. Cavanagh, J.F., Figueroa, C.M., Cohen, M.X., and Frank, M.J. (2012). Frontal theta reflects uncertainty and unexpectedness during exploration and exploitation. Cerebral Cortex *22*, 2575–2586.

89. Di Gregorio, F., Maier, M.E., and Steinhauser, M. (2018). Errors can elicit an error positivity in the absence of an error negativity: Evidence for independent systems of human error monitoring. NeuroImage *172*, 427–436.

90. Barrett, A.B., Dienes, Z., and Seth, A.K. (2013). Measures of metacognition on signal-detection theoretic models. Psychological Methods *18*, 535–552.

91. Rogasch, N.C., Sullivan, C., Thomson, R.H., Rose, N.S., Bailey, N.W., Fitzgerald, P.B., Farzan, F., and Hernandez-Pavon, J.C. (2017). Analysing concurrent transcranial

magnetic stimulation and electroencephalographic data: A review and introduction to the open-source TESA software. NeuroImage.

Control Analyses and Results

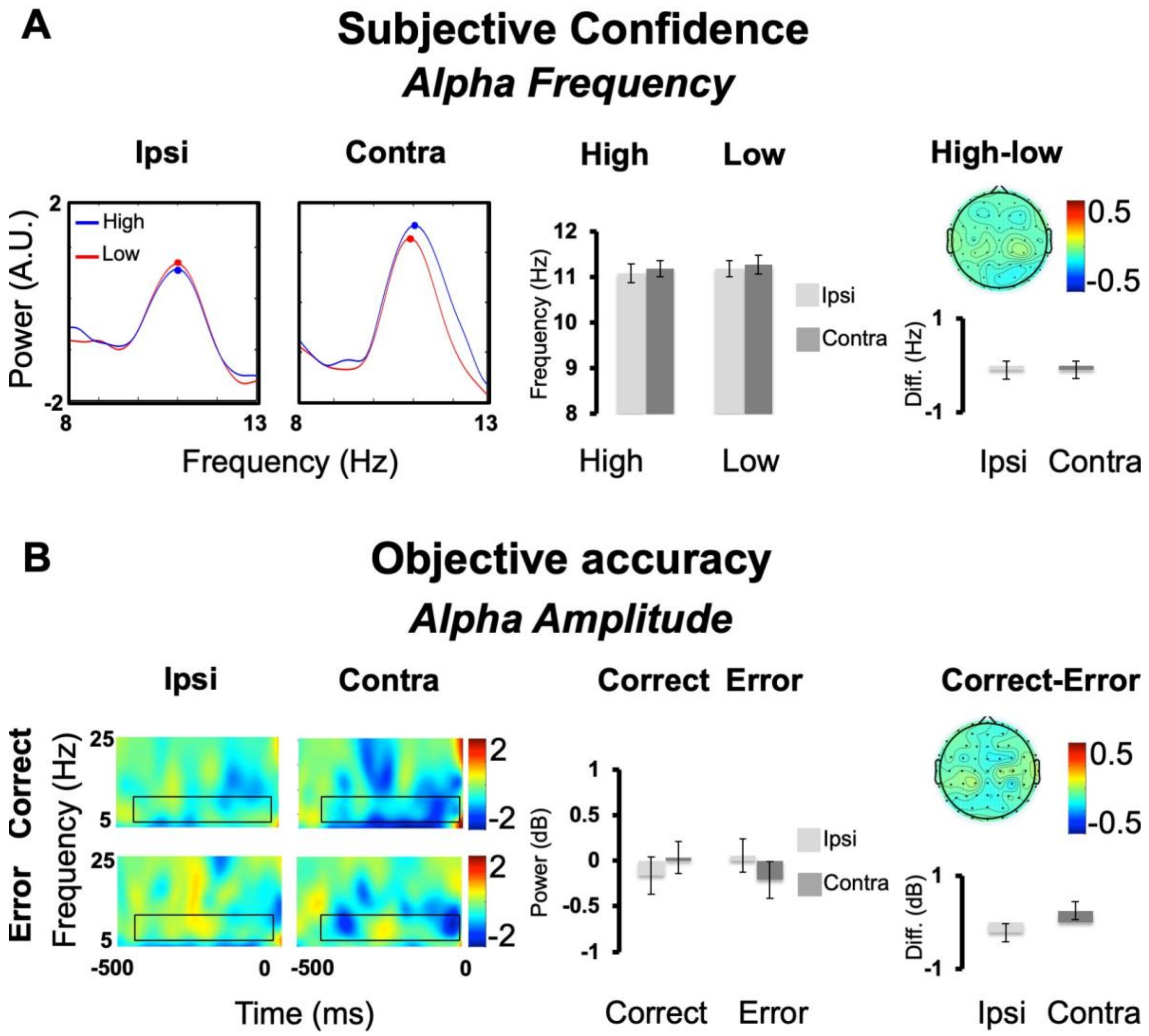

Figure S1. Results Experiment 1: Alpha-frequency and -amplitude in accuracy and confidence, related to Figure 2. A. Subjective Confidence. Averaged Alpha-frequency is represented as the z-scored mean power (10*$\log_{10}$[μv^{2}/Hz]) spectrum in the cue-stimulus time period for the contralateral and the ipsilateral electrodes and for Low and High confident trials within the alpha band. Bar graphs are reported for Low and High confident trials and for the difference in High-Low. Topography represents the difference High-Low (electrodes are flipped to represent contralateral activity in the right-hand side and ipsilateral activity in the left-hand side). No statistical effects reached significance (all Fs(1,23)<0.47; ps>.501; η_{ps}<.021), suggesting that alpha-frequency has no role in determining one individual confidence on their response. B. Objective Accuracy. Alpha-Amplitude is reported as time-frequency plots for the contralateral and the ipsilateral electrodes and for Correct and Error trials. Black boxes denote regions of statistical analyses (alpha band 7-13Hz). Bar graphs are reported for Correct and Error trials and for the difference in Correct-Error. Topography represents the difference Correct-Error (electrodes are flipped to have contralateral activity in the right-hand side and ipsilateral activity in the left-hand side). No statistical effects reached significance (all Fs(1,23)<2.133;

ps>.158; η_{ps}<.085), suggesting that alpha-amplitude has no role in determining objective accuracy. Error bars represent standard error of the mean A.U.=arbitrary units; Diff=difference; μv=microvolt; Hz=Hertz; ms=milliseconds; dB=decibel.

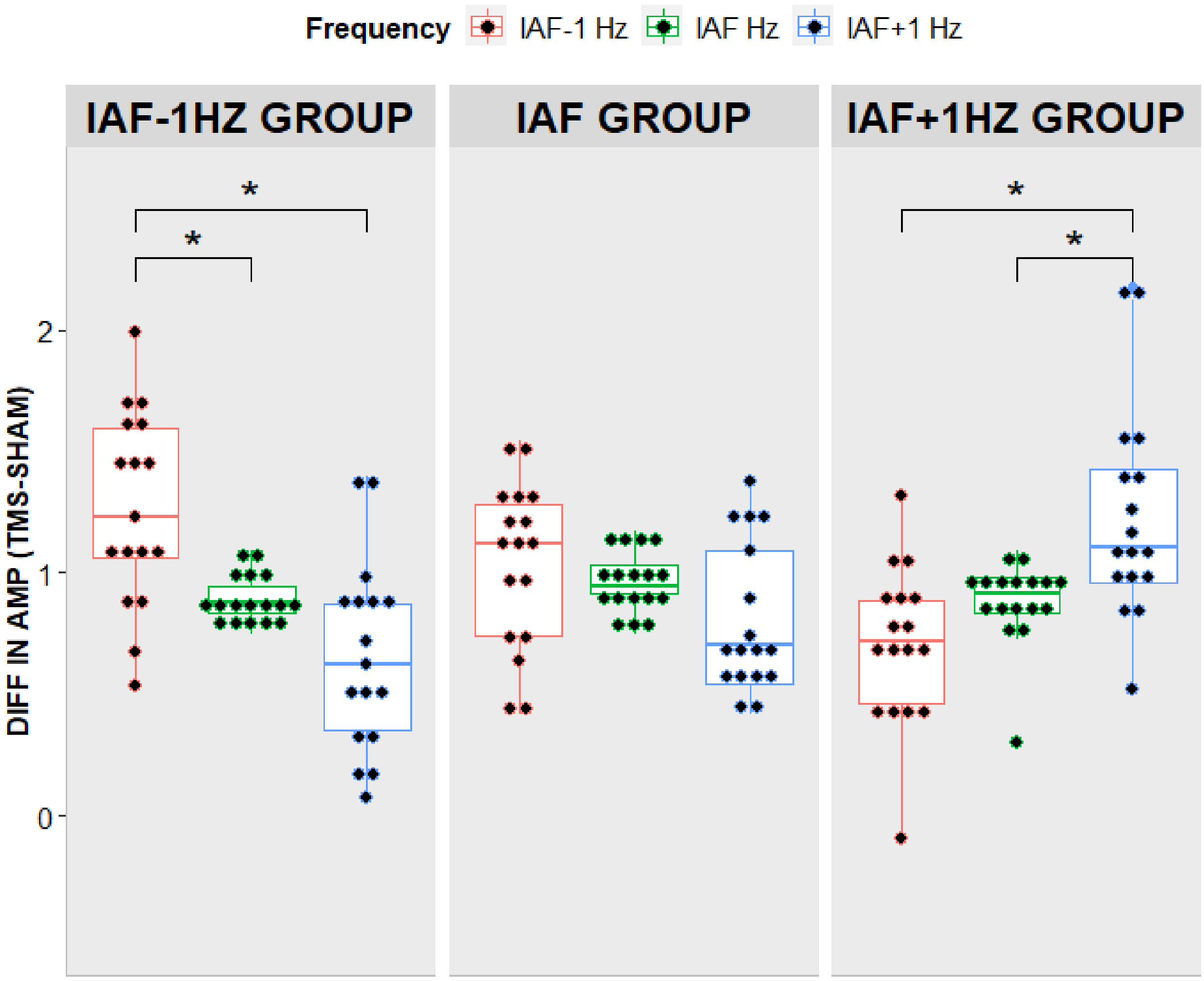

Figure S2. Results Experiment 2: Differences in alpha-amplitude across frequencies, Related to Figure 3. Box plots of differences in averaged alpha-amplitude between Active and Sham stimulation blocks for three experimental groups (IAF±1 and IAF groups) and for different frequencies (IAF1±Hz, and IAF frequencies). Horizontal lines represent the median value, while vertical lines represent the 25th and 75th percentile. Two-tailed t-tests are reported (*p<.05), showing highest differences between Active and Sham stimulation at the stimulated frequency both in the IAF-1 Hz and IAF+1 Hz groups. The effects gradually and significantly decreased at different alpha frequencies: all ts>2.45, all ps<.026, all ds>0.34. In the IAF group, there were no significant differences between flanker (higher and lower) alpha frequencies (F(2,32)=2.289; p=.150; η_p^2=.12), speaking in favor of a broadband entrainment effect in the alpha band for this group.

Control Methods

Experiment 2 and 3

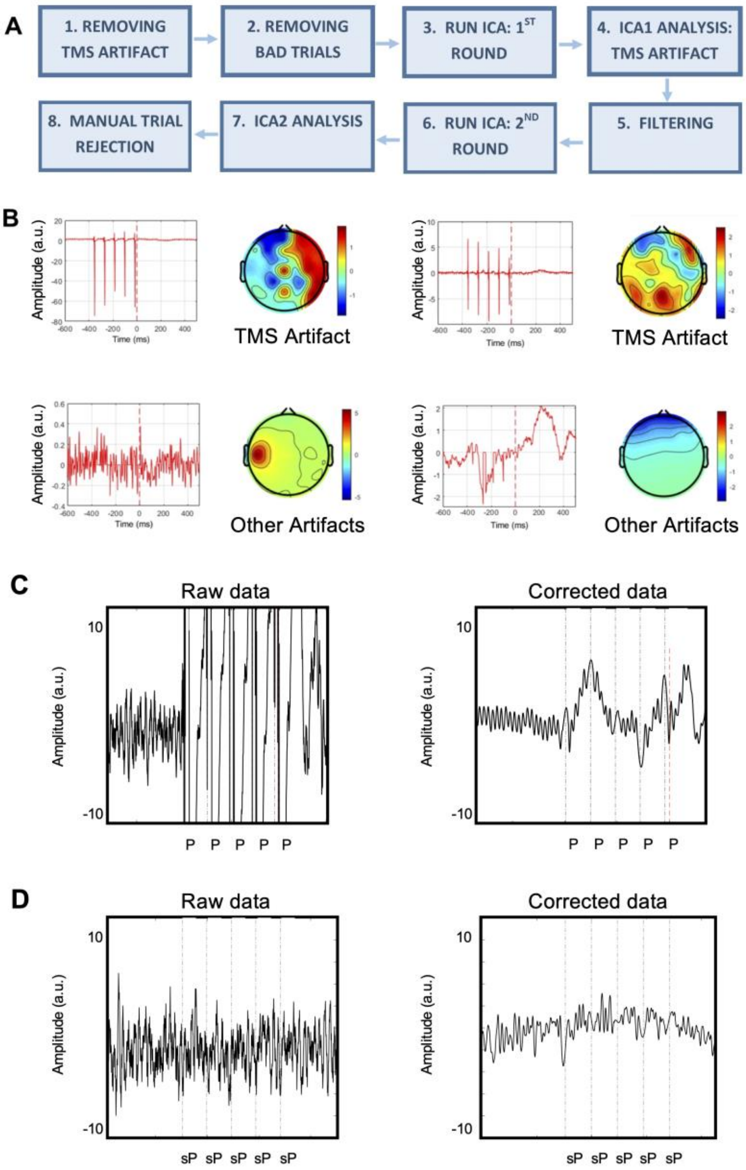

Figure S3. TMS artefact correction procedure, related to STAR Methods. A. EEG data processing workflow and pipeline for Experiments 2 and 3. B. Examples of artefact components removed in the first (TMS artefacts, upper row) and second (lower row) ICA analyses C. Effects of artefact rejection procedure on an active TMS condition. One second epoch of one participant before (Raw data) and after (Corrected data) the correction procedure. Dashed lines reflect Pre-stimulus TMS pulses (P) D. Effects of artefact rejection procedure on a TMS-artefact free signal. The procedure was applied to ensure that any effect we have observed could not be alternatively explained by a spurious effect of the cleaning protocol adopted. One second epoch of one participant before (Raw data) and after (Corrected data) correction procedure. It can be noticed that the artefact-removal procedure per se does not alter the underlying signal, confirming that the artefact-rejection procedure per se is not accountable for the modulation of the oscillatory activity. Dashed lines reflect simulated pulses (sP). ICA=Independent Components Analyses, A.U.=Arbitrary Units, ms=millisecond.